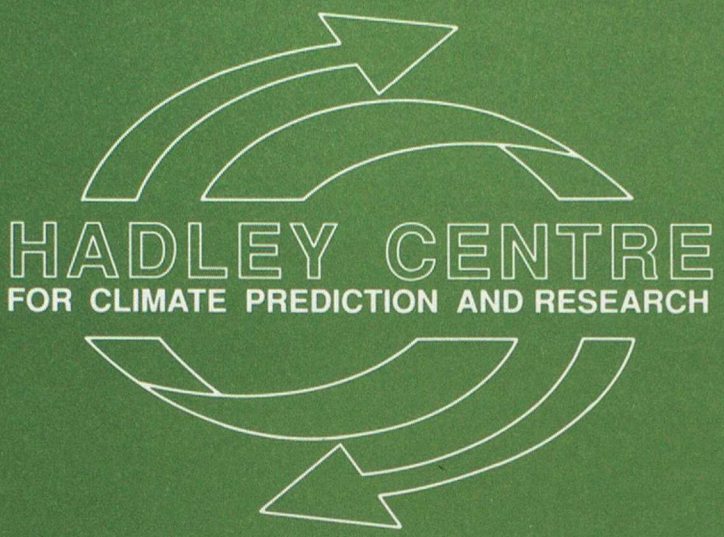

Parametrization of momentum transport by convection. II: Tests in single column and general circulation models.

by

D Gregory, R Kershaw and P M Inness

CRTN 64

December 1995

CLIMATE
RESEARCH
TECHNICAL
NOTE

Hadley Centre
Meteorological Office
London Road
Bracknell
Berkshire RG12 2SY

CLIMATE RESEARCH TECHNICAL NOTE NO. 64

PARAMETRIZATION OF MOMENTUM TRANSPORT BY CONVECTION. II: TESTS IN SINGLE COLUMN AND GENERAL CIRCULATION MODELS

by

D Gregory, R Kershaw and P M Inness

Hadley Centre for Climate Prediction and Research
Meteorological Office
London Road
Bracknell
Berkshire RG12 2SY

NOTE: This paper has not been published. Permission to quote from it should be obtained from the Director of the Hadley Centre.

Parametrization of momentum transport by convection. II: Tests in single column and general circulation models.

D.Gregory[12], R. Kershaw
and P.M. Inness
Meteorological Office,
London Road
Bracknell. RG12 2SY

December 1995

---

[1]Current Affiliation : ECMWF, Shinfield Park, Reading.

[2]Corresponding author

ABSTRACT

Diagnostics derived from cloud resolving model simulations in part I of this study (Kershaw and Gregory, 1995) relating to the vertical transport of horizontal momentum by convection are used to develop a parametrization of convective momentum transports for deep convection based upon the mass flux convection scheme discussed by Gregory and Rowntree (1990). The importance of cloud pressure gradients to the flow within the cloud is emphasised and a simple method of representing their effect suggested. The scheme is found to be able to reproduce the fluxes derived from the cloud resolving model studies where cloud organisation by the flow is unimportant. The scheme is also shown to represent some characteristics of up-gradient momentum transfer associated with organised convective systems. Inclusion of the parametrization in a version of the UK Met. Office Unified Model demonstrates that convective momentum transports play a large role in the momentum balance of the atmosphere. Generally simulation of the mean atmospheric circulation by the Unified Model is improved by the inclusion of such transports.

1. INTRODUCTION

In part I of this study, Kershaw and Gregory (1995) (referred to as KG95 hereafter), a cloud resolving model was used to estimate momentum transports due to deep convection for differing flow regimes and cloud organizations. Here those results are used to develop and validate a parametrization of convective momentum transports based upon the mass flux convection scheme of Gregory and Rowntree (1990). Such a methodology has several advantages over that using purely observational data. Together with estimates of the net transport of momentum, cloud resolving model simulations are able to provide details of the internal cloud structure, such as the variation of horizontal wind with height within the cloud. Also the structure and magnitude of the cloud pressure gradient can be estimated directly without appealing to a simple cloud model allowing representations for use in the convection scheme to be better validated.

In section 2 a brief description of the Hadley Centre Climate Model is provided while in section 3 modifications made to the convection scheme of Gregory and Rowntree (1990) to incorporate convective momentum transports are outlined. Section 4 reports single column model experiments parallel to those in KG95 with the aim of validating the convective momentum transports predicted by the scheme. The impact of the scheme on the circulation of the atmosphere as simulated by the global version of the Hadley Centre Climate Model is discussed in section 5.

2. DESCRIPTION OF SINGLE COLUMN AND GENERAL CIRCULATION MODELS

The model used in this study is the Hadley Centre Climate Model (a version of the UK Met. Office Unified Model described by Cullen (1993)). In part this is a development of the model used by Senior and Mitchell (1993), being of a grid-point type with 19 (irregularly spaced) levels in the vertical using a hybrid sigma/pressure co-ordinate. A conservative split-explicit integration scheme is used (Cullen and Davies, 1991), and cloud water and ice are included as prognostic variables. The model uses an Arakawa B-grid, pressure and thermodynamic variables being located at the centre of a grid box, velocity components at the corners.

The model configuration used in this study is that of HADAM2b (the "3rd Climate Version") described briefly by Hall et al (1995). The annual cycle of radiation is imposed on the model which employs an interactive radiation scheme (Ingram, 1993) incorporating the short wave cloud optical property scheme of Slingo (1989) using cloud water contents predicted by the cloud scheme of Smith (1990, 1994). Although the optical property scheme is strictly only applicable for water cloud it is also used in the model for ice clouds, although a different effective radius for the particles is assumed; 7μm for water clouds, 30μm for ice clouds. The radiation scheme is called every 3 hours in order to represent the diurnal cycle but the incoming solar flux is updated every time step to avoid discontinuities in surface properties. The boundary layer scheme is formulated in terms of conserved variables and so can represent both dry and cloudy boundary layers. It also includes a representation of non-local mixing (Smith, 1994). Mixing coefficients are stability dependent, using a moist Richardson number. A mass-flux convection scheme with stability dependent closure (Gregory and Rowntree, 1990) is included which includes a representation of deep convective downdraughts (Gregory and Allen, 1991). Further details of the scheme are given in section 3. Surface hydrology and a soil temperature model are also included (Warrilow et al (1986), Dolman and Gregory (1992)). Mean orography is used, together with a gravity wave drag scheme which accounts for the anisotropic nature of orography together with low level wave breaking associated with trapped lee waves and hydraulic jump like phenomena (Gregory et al, 1995). Roughness lengths for momentum are also increased over orography (Smith et al, 1995). At its lower boundary over ocean regions the model is forced with climatologically varying sea surface temperatures.

In this study both the global and single column versions of the HCCM are used. The single column version represents a single grid point of a GCM and is a useful test bed for the development of parametrizations before implementation in the full model, allowing detailed comparisons to be made with observations or diagnostics from detailed models.

3. A SCHEME FOR THE PARAMETRIZATION OF MOMENTUM TRANSPORTS

The convection scheme used here to represent the vertical transport of horizontal momentum by convection is based upon that described by Gregory and Rowntree (1990); the reader is referred there for details. The scheme is of a mass flux type with an instability closure. A bulk entraining cloud model is used although the scheme aims to represent an ensemble of clouds with differing zero buoyancy levels by allowing some of the ascending air to detrain below the zero buoyancy level of an undilute parcel (so called "forced detrainment"). Since the description of Gregory and Rowntree (1990) the scheme has been updated by the introduction of a downdraught parametrization (Gregory and Allen(1991), Gregory (1995)) based upon an inverted entraining plume with descending air being maintained at negative buoyancy by the evaporation of falling precipitation. This extension is briefly described below.

Kershaw and Gregory (1995) described the mass flux approach to the parametrization of convection, concentrating upon the vertical transport of horizontal momentum. There the equations were expressed in height co-ordinates. However as noted above the Unified Model is formulated in hybrid co-ordinates and the parametrization scheme is most readily expressed in pressure co-ordinates. Hence, analogous to equation (2) of KG95 and following similar notation, the effect of sub-grid scale circulations upon the large-scale wind can be written as;

$$Q3 = \frac{D\bar{V}}{Dt} = \left(-\frac{\partial \overline{u'\omega'}}{\partial p}, -\frac{\partial \overline{v'\omega'}}{\partial p}\right) \qquad (1)$$

where ω is the vertical p velocity, Dp/Dt.

Again following KG95 the vertical eddy flux of horizontal velocity can be expressed in terms of large-scale and cloud variables (their equation (7);

$$\overline{u'\omega'} = M^u(\bar{u}^u - \bar{u}) + M^d(\bar{u}^d - \bar{u}) \qquad (2)$$

where $\overline{\Phi^u}$ is the value of Φ in the updraught, $\overline{\Phi^d}$ the value of Φ within the downdraught and

M is the cloud mass flux. An analogous equation can be formulated for the meridional wind.

Hence the problem of determining the vertical eddy flux of horizontal momentum due to convection is reduced to estimating the mass flux within the upward and downward moving parts of the cloud together with the in-cloud horizontal velocities. This is done by modelling the updraught and downdraught as entraining plumes;

$$\frac{\partial M^u \bar{u}^u}{\partial p} = \epsilon^u M^u \bar{u} - \mu^u M_u \bar{u}^u + g\sigma^u \frac{\overline{\partial h}^u}{\partial x}$$
$$\frac{\partial M^d \bar{u}^d}{\partial p} = \epsilon^d M^d \bar{u} - \mu^d M_d \bar{u}^d + g\sigma^d \frac{\overline{\partial h}^d}{\partial x} \qquad (3)$$

and similarly for v. Here ϵ are entrainment rates, μ detrainment rates, h the height of a pressure surface and σ the cloud area.

(a) Updraught

For the updraught, equation (3) is discretised in the vertical following that in the original scheme described by Gregory and Rowntree (1990) (figure 1a). Entrainment rates are specified at levels k+1/4 and k+3/4, increasing linearly with pressure towards the surface with the aim of representing the more turbulent nature of shallow convection in the boundary layer. Two detrainment rates are specified, so-called "forced" detrainment (δ) associated with clouds within the assumed ensemble which have reached their zero buoyancy level and mixing detrainment (η) representing turbulent detrainment across the cloud boundary as the parcel ascends.

Starting from the lowest model layer, each layer is tested to determine if a parcel of air, given a small temperature perturbation, is positively buoyant when lifted to the next model level. Updraughts are initiated from the lowest such layer, the initial value of horizontal wind within the updraught being taken to be the grid box mean value. Entrainment and detrainment rates for horizontal momentum are the same as those for thermodynamic variables.

Equation (3) is similar to that for the vertical variation of thermodynamic variables within the

cloud, the cloud pressure gradient term replacing the latent heating term. However, unlike the latter, which is well related to the temperature and moisture content of the parcel, the cloud pressure gradient term is poorly understood theoretically. Early attempts to formulate parametrizations of convective momentum transports neglected this term (for example Shapiro and Stevens, 1980). However observational studies (e.g. Flatau and Stevens, 1987) and modelling studies (e.g. Gregory and Miller, 1989) indicate that this term plays an important part in determining the variation of horizontal velocity within the cloud as a parcel ascends. As commented upon in the introduction above, several previous studies have attempted to specify this term. The approach used in this parametrization is discussed in section 4.

The effect of the convection upon the large-scale momentum fields is estimated from equation (1) with the vertical eddy flux replaced by the approximate form of equation (2). An upstream difference is used. For zonal wind:

$$Q3_u^u = \left(\frac{\partial \bar{u}}{\partial t}\right)^u = -\frac{M^u_{k+1/2}(u_k^u - u_{k+1}^E) - M_{k-1/2}(u_{k-1}^u - u_k^E)}{p_{k-1/2} - p_{k+1/2}} \qquad (4)$$

and similarly for v. The eddy flux at top and base of the cloud layer is set to zero.

(b) Downdraught

Downdraughts are initiated from the highest model layer in which an equal mixture of updraught and environmental air, brought to saturation, is negatively buoyant after descent to the next lowest model level. As for thermodynamic variables, the initial value of horizontal momentum within the downdraught is the mean of the values within the updraught and cloud environment. Discretisation of equation (3) in the vertical is as described in Gregory (1995), summarized in figure 1b. Downdraught entrainment and detrainment rates for momentum are equal to those used for thermodynamic values being constant with height but enhanced as the downdraught crosses the freezing level, based on the observation that downdraughts in deep convective systems often form at this level. As the parcel descends, air warms by adiabatic compression which is compensated by the evaporation and melting of precipitation. When the downdraught reaches the surface, final detrainment is spread over

the lowest 100mb of the atmosphere. For further details the reader is referred to Gregory (1995).

The zonal and meridional winds in the cloud environment are modified using the same type of eddy flux formulation described above for the updraught.

$$Q3_u^d = \left(\frac{\partial \bar{u}}{\partial t}\right)^d = -\frac{M^d_{k+1/2}(u^d_{k+1}-u^E_k) - M^d_{k-1/2}(u^d_k - u^E_{k-1})}{p_{k-1/2}-p_{k+1/2}} \quad (5)$$

Fluxes at the top and bottom of the downdraught are set equal to zero.

4. SINGLE COLUMN MODEL TESTS AGAINST CLOUD RESOLVING MODEL DATA

One of the principal philosophies of the GEWEX Cloud Systems Study (GCSS) (Browning, 1994) is the use of data diagnosed from cloud resolving models to validate, and assist in the development of, parametrization schemes for general circulation models. KG95 has presented results from such a cloud model which here will be used to determine how successful the above mass flux parametrization is at predicting vertical momentum transports by deep convection and also to provide insight into how the effects of the horizontal pressure gradient term can be accounted for. Many of the experiments presented in KG95 are paralleled by ones using a single column version of the Unified Model described in section 2 above. The same initial profiles as used in the cloud resolving model simulations are used to initialise the single column model. Information on surface fluxes and cooling/moistening due to (implied) large scale ascent are also provided to the model, again being identical to those used in KG95. To eliminate cloud-radiation interactions and concentrate upon the performance of the convection scheme, the radiation scheme was not included in either model. All experiments presented are 10 hours in length using a 10 minute time step; results presented are averages over the whole of this period.

(a) COLD AIR OUT BREAK

The single column model was initialised with the sounding as used in the cloud resolving model simulation (see figure 1 of KG95). The initial wind field is uni-directional, increasing linearly from zero at the surface to 6km and is held constant above this at either 10 or 20ms^{-1} (see table 1 for an outline of the experiments carried out). The surface fluxes of latent and sensible heat were also varied as indicated in table 1. The cloud model simulations were three dimensional with a domain of 50km by 50km, 1km resolution in the horizontal and 500m in the vertical, the top of the model being at 15km. For further details the reader is referred to KG95.

(i) Performance neglecting cloud pressure gradients

So far in the formulation of the parametrization of momentum transports, the representation of the cloud pressure gradient term has not been considered in detail. As discussed previously, several studies have indicated the importance of this term. The single column model experiment discussed here (S32ncpg) serves to illustrate this. Experiment S32ncpg is parallel to experiment 232 of KG95 with a 10ms^{-1} linear increase in wind over the bottom 6km of the atmosphere and surface sensible heat/latent fluxes of 100 and 400Wm^{-2} respectively but the effects of the cloud pressure gradient term are neglected in the parametrization of convection.

From equation (2) the vertical eddy flux of momentum is dependent upon the convective mass flux and in-cloud velocity. Figure 2 compares the vertical profile of convective mass flux from the convective parametrization scheme with that diagnosed from the cloud model simulation. For the purposes of defining updraught characteristics from the cloud resolving model, a grid point was defined to be part of an updraught if the vertical velocity exceeded 1ms^{-1} and cloud water or rain water was greater than 0.1g/kg. Similarly, downdraught points were taken to be those at which air was descending in the presence of rain water exceeding 0.1g/kg. Deficiencies are seen in the mass flux predicted by the parametrization, with the updraught mass flux peaking at around 5km, whereas the cloud simulations suggest the mass flux peaks at 1.5km. However peak values are of similar magnitude and throughout much

of the upper cloud layer (above 3.5km) values are similar. For the downdraught both the cloud model and parametrization show an increase in mass flux towards the surface. However the downdraught mass flux is approximately one third that suggested by the cloud model simulation.

The form of the mass flux profile for the updraught is typical of that predicted by entraining plume models of convection. Several explanations may account for the difference between the mass flux profiles diagnosed from the cloud model and predicted by the parametrization. Firstly although the process of "forced detrainment" is an attempt to compensate for the use of a single convective plume in the parametrization scheme, allowing convection to continue upwards even though the parcel becomes negatively buoyant before the level to which an undilute parcel can ascend, it may not provide an adequate description of the distribution of the top heights of clouds within the simulated cloud ensemble. A contributing factor to this may be the neglect of water loading effects in the estimation of parcel buoyancy, although the use of high entrainment rates near the base of the convective plume may compensate for this. Secondly the entrainment formulation used in the plume model may not be appropriate for deep convection. The smallness of the downdraught mass flux may imply that its initial value needs to be increased or the entrainment formulation modified. These areas of the parametrization require further investigation which is beyond the scope of this paper. Initial studies suggest a closer fit between the updraught mass fluxes is possible when the updraught entrainment rates are increased below 800mb and set to zero above this level (not shown). It is not clear how valid this treatment would be when the scheme is used over a wide range of conditions, as is the case in a GCM.

Considering the incloud horizontal velocity (v) (figure 3), the impact of the neglect of the cloud pressure gradient by the parametrization is clearly seen. Whereas incloud velocities in the cloud resolving models updraughts deviate only by 1-2ms^{-1} from the large-scale average, values predicted by the parametrization are up to 5ms^{-1} slower than those of the large-scale environment of the clouds. Horizontal velocities within the downdraught are also close to the environmental value in the cloud simulation, but in the parametrization vary little with height from their initial value, being greater than the large-scale value below 2.5km.

Figure 4a compares the vertical eddy flux of horizontal momentum calculated using equation (2) for the parametrization with that from the equivalent height formulation for the cloud model (equation (7) of KG95). The vertical transport of momentum by the updraught is generally overestimated by the parametrization above 2km, due to the larger cloud-environment wind difference noted above. Below this height, the momentum flux in the cloud model is greater due to the larger mass flux in this region. The contribution from the downdraught to the net momentum flux is small above 5km but is of a similar, but opposite, magnitude to the updraught flux in the lowest kilometre. The parametrization gives a flux of opposite sign to that found in the cloud model below 3km due to errors in the downdraught horizontal wind discussed above. The net vertical eddy momentum flux (figure 4b) estimated by the parametrization is greater than that diagnosed from the cloud model up to 6km, with the level of the maximum value being 1km lower. Above the maximum, the parametrized curve falls off more rapidly with height, a consequence of the plume model underestimating the top height of the convecting layer by 2km. Note that combining the updraught and downdraught fluxes estimated from the cloud model simulation gives a positive flux below 1km. This contrasts against the total flux shown in figure 10 of KG95 which is negative at all heights. The discrepancy arises from the neglect of the environmental term in equation (3) of KG95 in deriving the net flux of figure 4b.

The larger vertical gradients in the parametrized eddy flux profile lead to an overestimation of the deceleration of the flow above 4km by $3ms^{-1}$ per day (see figure 8 later - Q3 with both convective and boundary layer contributions combined). This causes the large-scale horizontal velocity to deviate further from the initial wind profile than the domain averaged horizontal velocity in the cloud model simulations (figure 3). The wind speed in the lowest kilometre of the domain of the single column model is larger than in the cloud resolving model. The larger westerly accelerations predicted by the parametrization are mostly due to the boundary layer scheme (85% of the acceleration in the lowest model layer). These larger values near the surface in the single column model may be a consequence of the much finer resolution in this region. The height of the lowest model layer in the single column model is 25m compared to 250m in the cloud resolving model. Thus the boundary layer in the cloud model is not well resolved. Future work, of the type described in this paper, will require better matched vertical resolution between models within the boundary layer.

(ii) Parametrization of cloud pressure gradients

Thus far, the results shown indicate that the parametrization scheme is able to capture the form of the downgradient momentum flux associated with convection in a (simulated) cold air outbreak. However the magnitude of the convective forcing upon the horizontal wind is overestimated as the incloud horizontal velocities predicted by the parametrization differ from the large-scale values by more than predicted by the cloud model.

Several recent parametrizations of convective momentum transports have attempted to include the effects of cloud pressure gradients upon horizontal velocity of a parcel as it ascends through a convective cloud. König and Ruprecht (1988) and Zhang and Cho (1991a) both attempted to formulate an expression for the pressure gradient term through consideration of a simple model of flow around a convective tower. Others have tried a simpler and rather more empirical approach, increasing the entrainment and detrainment rates used in equations (3) above those used for thermodynamic quantities (Nordeng (1995), ECMWF convection scheme) implying enhanced mixing between the cloud and environment. However, the suitability of these formulations has only been addressed by the comparison of Q3 predicted by the schemes with values estimated from budget studies using observational data. It is usually thought that large errors exist in these observational estimates of Q3. For example Zhang and Cho (1991b) estimate that errors in Q3 derived from GATE data are equal to half of the maximum values. Here the cloud resolving model simulations allow the pressure gradient term to be diagnosed directly and so a more thorough comparison can be made. Also the form and magnitude of this term can be studied over a wide range of different flow conditions.

Figure 5 shows the vertical structure of the pressure gradient term for the updraught from experiment 232 and experiments 233, 236 and 237 of KG95 (see table 1) in which either the shear in the lower part of the domain has been doubled (to $20ms^{-1}$ over 6km) and/or the surface latent heat flux doubled (to $800Wm^{-2}$). The net condensational heating is well related to the net surface forcing and a doubling leads to an increase in the surface precipitation by approximately a factor of two. Previous studies (for example Gregory and Miller, 1989) have shown that the condensational heating due to convection can be approximated as

$(M^u+M^d)\partial\theta/\partial p$ (so called "compensating subsidence"). Hence a doubling of convective heating is approximately equal to a doubling of convective mass flux. This is confirmed by comparison of the mass fluxes diagnosed from the cloud resolving model simulations 232 and 236 (see figure 7 of KG95).

In figure 5, the peak magnitude of the pressure gradient term doubles as the shear across the cloud layer is doubled (experiments 232 and 233). Similar behaviour is also found when the surface latent heat flux (and so the convective mass flux) is doubled (experiments 232 and 236) while when both shear and surface latent heat flux are doubled the peak magnitude of the cloud pressure gradient increases by about a factor of four.

This behaviour suggests that a simple parametrization of the form,

$$g\sigma^u\frac{\overline{\partial h}^u}{\partial x}=C^uM^u\frac{\partial\bar{u}}{\partial p} \tag{6}$$

where C^u is a coefficient (to be determined), may be appropriate for the updraught. Such a parametrization does have some theoretical basis. Considering the momentum equation for the plume model used to describe the updraught in the parametrization,

$$M^u\frac{\partial\bar{u}^u}{\partial p}+\bar{u}^u\frac{\partial M^u}{\partial p}=\epsilon^uM^u\bar{u}-\mu^uM^u\bar{u}^u+g\sigma^u\frac{\overline{\partial h}^u}{\partial x} \tag{7}$$

Using the mass continuity equation for the updraught,

$$\frac{\partial M^u}{\partial p}=\epsilon^uM^u-\mu^uM^u \tag{8}$$

to substitute into the l.h.s of equation (7) gives after rearrangement,

$$M^u\frac{\partial\bar{u}^u}{\partial p}=\epsilon^uM^u(\bar{u}-\bar{u}^u)+g\sigma^u\frac{\overline{\partial h}^u}{\partial x} \tag{9}$$

Assuming that the entrainment term is small, and also that the vertical gradient of u within the cloud is close to that within the cloud environment (reasonable from figure 3),

$$M^u \frac{\partial \bar{u}}{\partial p} \approx g\sigma^u \frac{\overline{\partial h}^u}{\partial x} \qquad (10)$$

This analysis suggests that the coefficient C should be close to unity although as the vertical gradient of horizontal wind within the cloud is less than in the cloud environment (by around 20% in this case - see figure 3) in reality a value less than unity might be expected. A similar analysis can be carried out for the meridional velocity and also the downdraught, with the same form resulting.

iii) Inclusion of cloud pressure gradient

Experiment S32 was carried out parallel to S32ncpg but with the cloud pressure gradient term included in the convection scheme as described above. Reasonable agreement was found between the parametrized pressure gradient term and that diagnosed from the cloud model if the coefficient in equation (6) was set to 0.7 for both the updraught and the downdraught (figure 6). The parametrized pressure gradient is rather noisy in the vertical, a consequence of the parametrization scheme enhancing the vertical gradient of horizontal velocity in the mid-levels due to excessive deceleration of the flow and also the underestimation of the cloud top height (see figure 5). However, the general structure of the term is reasonably captured, for both the updraught and, below 5km, the downdraught.

Incloud velocities are in better agreement with those diagnosed from the cloud resolving model simulation (figure 7a and b). Differences between the updraught velocities and those of the large-scale flow predicted by the parametrization scheme are now smaller than predicted by the cloud model analysis, perhaps a consequence of the cloud pressure gradient term being larger than that in the cloud model simulation. Downdraught horizontal velocities still exceed those of the large-scale flow in the lowest 3km of the model domain, again leading to the parametrized vertical eddy momentum flux associated with the downdraught having the wrong sign. However this has little consequence for the net momentum transport of the clouds as the flux of momentum associated with the downdraught is much smaller than that of the updraught (see figure 4a previously). The net Q3 predicted by the parametrization is in better agreement with that diagnosed from the cloud model throughout much of the

cloud layer when the effects of the cloud pressure gradient are included. (figure 8)

It is important that parametrizations are valid over a wide range of conditions in which convection may exist and so several companion experiments were carried out for this case in which the shear and surface latent heat flux were doubled (see table 1). Figure 9 shows the parametrized pressure gradient term for the updraught and downdraught compared to those diagnosed from the cloud model for experiment S37 and 237 (of KG95) in which the shear has been increased to $20ms^{-1}$ over the lowest 6km of the domain and the surface latent heat flux increased to $800Wm^{-2}$. Again the parametrization fits the cloud model result reasonably well, although the magnitude is underestimated for the downdraught. Horizontal velocities within the updraught and downdraught also follow those diagnosed from the cloud model, although again downdraught velocities exceed domain mean velocities. This leads to the momentum flux associated with the downdraught being of opposite sign of that found in the cloud model. The structure and magnitude of Q3 (figure 10) is well captured by the parametrization, although again transports due to boundary layer processes lead to excessive accelerations in the lowest kilometre of the single column model domain.

(b) TROPICAL CASE

(i) Unorganised cloud system

The above results suggest that the parametrization scheme described herein is able to represent downgradient transports of momentum in a case with linear uni-directional shear (of varying magnitude) when clouds have little organization. However when used in a general circulation model the scheme will encounter a wide range of vertical wind shears. Here, the performance of the parametrization is studied for a case of convection developing in the vicinity of a low level jet, experiments paralleling the tropical case of KG95 (see table 2). Profiles of temperature and moisture are based upon those found during the GATE experiment over the eastern tropical Atlantic and the wind profile is uni-directional with a westerly jet in the lower troposphere. As well as surface forcing, the single column model was also forced with cooling and moistening terms representing the effect of large-scale motion in the ascending branch of the Hadley circulation (figure 11). Although the shape of these profiles

is idealised, peak magnitudes are typical of those found during periods of active convection over the GATE experimental area. The cloud model simulation here is three dimensional with the same domain as in the cold air outbreak case, but extending up to 20km in the vertical to accommodate the deeper clouds which form. Although the low level jet is similar to those associated with the development of a squall line, no such organization developed in the simulation. Hence the case is primarily one of downgradient momentum transport.

The convective vertical mass flux from experiment S35 (parallel to cloud resolving model experiment 235) is shown in figure 12. The discrepancies in mass flux between that predicted by the cloud model and the parametrization are similar to those seen in the cold air outbreak case. Although the shape of the downdraught mass flux profiles agree, the magnitude of the parametrized mass flux is only half that found in the cloud model. The updraught mass flux profile predicted by the parametrization peaks at 4km. Sensitivity studies with the parametrization scheme have shown that if the downdraught mass flux is increased to values similar to those of the cloud model in the lower troposphere, the updraught mass flux increases to compensate the increased cooling tendency due to the downdraught , thus allowing the convection scheme to balance the cooling due to large-scale forcing.

Agreement between the parametrized pressure gradient term and that diagnosed from the cloud model simulation is again encouraging (figure 13). One might not expect the same coefficient in equation (6) to be valid in such a different situation. However with a value of 0.7, as above, the magnitude of the pressure gradient term is well captured by the parametrization. For the updraught, the vertical structure of the pressure gradient term is well captured below 7km, although it is shifted downwards by 1km and falls off too rapidly with height. If only the last 5 hours of the simulation are considered (not shown) better agreement between the parametrization and cloud model is found in terms of the vertical location of the maxima and minima of the profiles, although again the parametrized pressure gradient term falls off too rapidly in the vertical. For the downdraught, the pressure gradient parametrization predicts the vertical structure of the term well below 5km, the region in which downdraughts associated with falling precipitation usually occur.

Figure 14 shows the horizontal wind in the updraught and downdraught for this case. The

cloud pressure gradient term is again important in determining the variation of horizontal wind within the cloud, bringing values in the updraught closer to the large-scale value than entrainment alone (not shown). However, the difference between the updraught and large-scale horizontal velocities is smaller than that found in the cloud model (below 8km), leading to an underestimate in the negative momentum flux below 4km. Above this height the momentum flux associated with the updraught is overestimated, the smaller velocity difference being compensated by the larger mass flux predicted by the parametrization scheme. The net effect of the convective momentum transport (Q3 - figure 15) predicted by the parametrization is in good agreement with that diagnosed from the cloud model, being down gradient, with the shear in the upper and lower parts of the jet being reduced together with a reduction in the peak wind speed in the jet core. Neglect of the cloud pressure gradient term in the momentum budget of the plume model used by the parametrization leads to an overestimation of the upward transport of momentum and to the upper flow being accelerated to the east too strongly above 5km.

(ii) Impact of cloud organization

The cloud simulation above was three dimensional and the cloud was not found to exhibit any strong degree of organization. Running this case with a two dimensional cloud resolving model (with a 500km domain) produced a squall line type system (see KG95). Figure 15 shows Q3 diagnosed from this simulation, demonstrating upgradient transports of momentum, with the initially stationary upper level flow being accelerated to the west (figure 17). Clearly the parametrization above does not capture this feature. A key difference between the two dimensional and three dimensional cloud resolving model simulations is the pressure gradient across the updraught (figure 16). In the squall line simulation its vertical structure is again well related to the vertical gradient of the large-scale horizontal velocity (figure 17). However its magnitude is much larger than in the three dimensional simulation (by a factor of 3-4), although this may be overestimated due to the two dimensional nature of the simulation. The large pressure gradient in the upper part of the jet causes the horizontal velocity within the updraught to become negative, leading to the upgradient transport of momentum.

The increase in the pressure gradient term could be accounted for in the parametrization by a simple increase of the coefficient in equation (6). Increasing this coefficient by a factor of 3 (from 0.7 to 2.1) gave a reasonable estimate of the structure of the pressure gradient across the updraught below 5km (not shown) but over estimated its magnitude in the upper troposphere (with a peak value of 70ms^{-1} per day at 9km). Increasing the coefficient to 1.4 (experiment S34), although giving an underestimate of the term in the lower troposphere (figure 16) allows the incloud flow of the parametrization to develop characteristics which are similar to that diagnosed from the cloud resolving model in the upper troposphere.

Horizontal velocity within the updraught diagnosed from the cloud model is less than the large-scale average velocity (figure 17), implying the updraught tilts against the low level shear. The large pressure gradient in the upper part of the low level jet (4-5km) accelerates the incloud flow to the west and it becomes easterly above 5km. The updraught vertical momentum flux is negative throughout the cloud layer and above 7km the large-scale flow is accelerated westward while the strength of the low level jet is maintained. These characteristics are typical of upgradient transports associated with tropical squall lines (see KG95 for further discussion).

In the parametrization, horizontal velocity within the updraught is also less than the large-scale value for the parametrization above 5km, implying a westward tilting updraught (assuming the cloud system is propagating to the east with the speed of the jet maximum). Beneath this height the updraught horizontal velocity is faster than the large-scale flow and the updraught slopes up the low level shear. Such a flow configuration leads to a negative vertical momentum flux in the upper part of the cloud with the initially stationary large-scale flow accelerated westward associated with upgradient transport. However below 6km the updraught momentum flux is positive, the opposite of that found in the cloud model simulations, a consequence of the updraught horizontal wind speed being faster than the large-scale flow. In this region momentum transports are downgradient, the strength of the jet maximum being reduced to 6.5ms^{-1} (averaged over the 10 hours of the simulation) from its initial value of 10ms^{-1}, while only falling to 9ms^{-1} in the cloud resolving model simulation.

Although there are deficiencies in the parametrized momentum transport associated with the

squall line, the above results suggest that it may be possible for such a mass flux parametrization to account for upgradient momentum transport. Clearly more work is required before it could be claimed that the parametric representation was adequate, especially on improving the characteristics of the incloud flow so that it better matches those diagnosed from the cloud model. Some criteria would also need to be developed to determine when, for example, a higher value for the coefficient of the parametrized pressure gradient term should be used. This will be briefly discussed later (section 6).

5. IMPACT OF CONVECTIVE MOMENTUM TRANSPORTS ON A GCM SIMULATION

Many previous observational and modelling studies have shown the importance of convective momentum transports to the general circulation. However, because of the relatively poor validation of suggested scheme against observational data compared to that carried out for the impact of convection upon temperature, few operational models have implemented such parametrizations.

Here the sensitivity of the Hadley Centre Climate Model to the inclusion of convective momentum transports is considered. As described in section 2 the model uses an Arakawa B-grid. In the convection scheme, wind components are interpolated on to the centre of the grid box, tendencies of u and v being interpolated back to the velocity points before these are updated. Comparison is made between two three year long simulations, the control (simulation C), in which convective momentum transports are not included, and simulation M in which they are. In simulation M, the pressure gradient term is accounted for in the momentum budget of the cloud as described above, with the coefficient in equation (6) being set to 0.7. No attempt is made to account for the organisation of convection and so only down gradient transports are represented. For brevity, results for northern winter (December/January/February (DJF)) are concentrated upon although the impact of convective momentum transports upon the northern summer (June/July/August (JJA)) circulation is briefly illustrated.

The above results and discussion have pertained only to the problem of representing momentum transports associated with deep convection. In the global model, shallow convection (within the boundary layer) can also exist. As the pressure gradient term results from the blocking of the flow by the convective plume, it is assumed that such an effect is small for shallow convection due to individual clouds having a small horizontal extent. Hence the cloud pressure gradient term is only applied to cases of deep convection. The performance of the scheme with regard to momentum transport associated with shallow convection has yet to be fully validated against detailed models and observational data. However, in a further integration of the HCCM in which only shallow convection was allowed to mix momentum in the vertical, the atmospheric flow was found to be similar to that of the control integration. This suggests that mixing of momentum by shallow convection is of little importance. However this may be a consequence of the use of a boundary layer scheme which represents rapidly mixing terms and also is formulated in terms of moist conserved variables and so is able to represent mixing in cloudy boundary layers (Smith, 1994). In a model in which only local dry mixing was represented by the boundary layer scheme, the convection scheme may play a greater role in representing the effects of clouds in the boundary layer.

Considering the zonal mean momentum balance,

$$\frac{\partial \bar{u}}{\partial t} = -\left(\frac{\partial \bar{u}}{\partial t}\right)^{DYN} + \left(\frac{\partial \bar{u}}{\partial t}\right)^{BL} + \left(\frac{\partial \bar{u}}{\partial t}\right)^{GWD} + \left(\frac{\partial \bar{u}}{\partial t}\right)^{CONV} \qquad (11)$$

where DYN, BL, GWD and CONV denote dynamical processes, boundary layer turbulence, gravity wave drag and convection. In the seasonal mean around the time of the winter and summer solstice (DJF and JJA) the time rate of change of zonal mean u is small and tendencies between these forcings are in approximate balance.

In the control experiment (C) only the boundary layer and gravity wave drag schemes together with dynamical processes modify the model's winds. Figure 19 shows the zonal mean forcing of the zonal flow by these processes for experiment C for DJF. In the lower troposphere the dominant terms in the momentum budget are those due to dynamical

processes and boundary layer turbulence. In the upper troposphere of the northern hemisphere, gravity wave drag balances the acceleration due to a northward flux of zonal momentum. Tendencies in the tropics and southern hemisphere above the boundary layer are less than $1 ms^{-1}$ per day.

Inclusion of convective momentum transport (experiment M) introduces an additional forcing into the budget and changes the nature of the equilibrium (figure 20 - DJF). Boundary layer tendencies are similar to those in the control simulation, tendencies due to convection being much smaller than those due to the boundary layer scheme below 900mb. Consideration of the integration in which only shallow convection mixed momentum in the vertical suggests that half of the contribution from convection below 900mb is due to shallow convection. The contribution of the dynamics tendency to the balance is reduced near 45°N around 800mb as convection also provides a westerly acceleration in this region (associated with the mixing down of faster moving air to the 800mb level by deep convection). In the upper troposphere of the northern mid-latitudes, convective drag is approximately half that associated with gravity wave drag. However the level of maximum convective drag is lower than that associated with gravity wave drag (between 200 and 300mb) being in the jet core rather than on the upper northward flank of the jet. In the southern hemisphere, the dynamics now provides a net westerly acceleration compensating convective drag in the upper troposphere. In the central ITCZ convection provides a westerly drag on the upper level easterly flow flanked by easterly accelerations to the north and south, with the opposite pattern being seen in mid-levels. Neglect of the pressure gradient term in the cloud momentum budget of the parametrization roughly doubles the magnitude of the convective tendencies although the pattern remains similar (not shown) with the contribution of other processes increasing to compensate.

The contribution of convective momentum transports to the meridional momentum budget (figure 21) acts to slow down the Hadley circulation with northward accelerations in the northern hemisphere inflow region, southward accelerations in the vicinity of the main outflow region in the upper troposphere (see later for further discussion). These tendencies are balanced in the seasonal mean by dynamical processes above the boundary layer, while within the boundary layer convection acts in the same sense as the boundary layer scheme.

Hence tendencies of velocity due to the latter are reduced with the introduction of convective momentum transports.

In order to achieve the differing equilibrium between the tendencies of zonal wind shown above when convective momentum transports are included, the mean wind structure of the model must adjust. Figure 22b shows the zonal mean difference of u for the simulations C and M from a climatology based upon ECMWF analyses between 1987 and 1993, again for DJF. Errors in the simulation of u are reduced when convective momentum transports are included, especially in the tropics and mid-latitudes (figure 22c). In the tropics the westerly bias of the flow in the mid-levels is reduced (from a maximum of $6ms^{-1}$ to $2ms^{-1}$), although the flow near 200mb has been slowed too much and is too easterly. The magnitude of the easterly error near 100mb has been reduced. In the southern hemisphere, winds are closer to the climatological values below 200mb south of 40°S although the core jet strength is still excessive. Improvements in errors associated with the mid-latitude winter hemisphere jet are also seen due to a slight southward shift of the jet maxima in the eastern Pacific and eastern Atlantic.

In the zonal mean meridional circulation (figure 23), the Hadley circulation is reasonably captured by both simulations. Changes in the circulation with the introduction of convective momentum transports are small apart from in the outflow region in the upper troposphere. Although the control simulation captures the maximum value of the northerly flow well, it is placed too high at 150mb rather than near the 200mb level as in the ECMWF data. Introduction of convective momentum transports appears to correct the level of maximum outflow but increase the maximum wind speed. This is in contrast to the southerly acceleration provided directly by the convection scheme and illustrates that the changes in the structure of the model's wind field described when convective momentum transports are introduced into the model are not, on the seasonal timescale, direct responses to the forcing but represent an adjusted balanced state in which the forcing of the winds by different processes are in an approximate equilibrium.

Convective momentum transports also have a significant impact upon the zonal flow during northern summer (JJA - figure 24). The control simulation has a large easterly error in the

tropical upper troposphere which is reduced on the introduction of convective momentum transports, as is the westerly error between 500 and 250mb centred on the equator. Wind errors in the northern and southern mid-latitudes associated with jets are also reduced except around 45°S.

These results indicate that convective momentum transports do play a significant role in the momentum budget of the atmosphere, in agreement with earlier studies. The changes in both the zonal and meridional wind reported are similar to those described by Zhang and McFarlane (1995) using a mass flux convection scheme with momentum transports in the Canadian Climate Centre (CCC) model. The magnitude of their estimates of Q3 were similar to those predicted here, as were the resulting changes in the zonal velocity. They too noted an increase in the intensity of the Hadley circulation and following Helfand (1979) they attributed this to the response of the meridional circulation to the forcing of zonal momentum by convection via the Coriolis force. Such an interpretation is consistent with the results presented here, the westerly acceleration of the 200mb flow at 10°N tending to give an enhanced southerly flow in the upper levels. This should be contrasted with the work of Tiedtke (1989) who found that convective momentum transports had little impact upon the divergent flow of a version of the ECMWF model.

6. DISCUSSION

This paper, together with Kershaw and Gregory (1995), has attempted to address the question of how convective momentum transports should be represented in large-scale models. It is not the first to do so. As discussed there have been several previous papers over the past twenty years which have studied the importance of this process and have suggested various methods by which it may be parametrized. Over this time several of the important issues involved in the problem have become clear, for example the important modifying effect of across-cloud pressure gradients on the incloud flow. However, partially due to the poor nature of observational estimates of Q3 and the known complexity of convective systems, with their down- and up-gradient transports of momentum, little confidence has been gained in the methods developed, resulting in convective momentum transports being wholly

neglected in GCMs or included for pragmatic reasons rather than a belief that they improve the physical basis of a model.

This study has used a method which will hopefully allow better convection schemes to be developed, namely using cloud resolving model simulations to provide data against which parametrizations can be compared. The advantages of the method are clear, details of the flow inside the cloud being better defined than is possible from current observational studies, as are the structure, magnitude and variation of the forcings which determine the cloud characteristics. However, the success of the method relies upon the accuracy of cloud model simulations. This is acknowledged by the GCSS community (Browning, 1994) who place a great deal of emphasis upon model validation and intercomparison as a first step in developing parametrizations. This is of course a correct procedure. The model used in this study has been validated against observations for several cases of deep convection (Dharssi et al (1995), Brown and Swann (1995)). Kershaw and Gregory (1995) also comment briefly on the accuracy of the simulation used here. For the tropical case the predicted convective mass flux profile is similar to that found in other models and observational studies. For the two-dimensional case the vertical structure of Q3 is similar to that obtained from other modelling and observational studies (e.g. LeMone, 1983). Whilst it is difficult to validate the cold air out break case, the results appear relatively insensitive to changes in horizontal and vertical resolution. Thus some confidence can be placed upon the cloud resolving model results used in the development of the parametrization scheme. However the work presented here is probably best seen as preliminary, serving to illustrate the methodology of using cloud resolving models to improve parametrization for large-scale models rather than providing a fully accurate representation.

Even with this caveat, the parametrization scheme described seems able to capture both the magnitude and vertical structure of the momentum transports associated with deep convection. This has been demonstrated for two widely differing flow regimes in which downgradient transport of momentum by convection occurs. Using diagnostics from the cloud model, a simple (compared to other recent parametrizations, e.g. Zhang and Cho (1991b)) representation of the effect of across-cloud pressure gradients upon the incloud flow has been formulated. Although simple this important part of the scheme has been well validated, being

found to capture both the vertical variation and magnitude of this term in the cloud momentum budget. It is of interest that using the same coefficient in the parametrization of the pressure gradient term (see equation (6)) gave acceptable results over differing flow configurations when clouds showed no strong degree of organization.

Comparison of cloud model and parametrization predictions also indicates areas where the simple cloud model used in the convection scheme needs improvement. Better entrainment and detrainment rates need to be specified in order to bring about a better description of the vertical variation of the updraught mass flux. For the downdraught, although the shape of the mass flux profile was reasonable, its strength was underestimated. Initial studies indicate that improvements are possible on a case by case basis but a general formulation has yet to be developed. Also the current downdraught formulation gives a flux of momentum of the wrong sign compared to the cloud model. This is due to the horizontal velocity within the downdraught of the parametrization being incorrectly forecast, indicating that an improved model may be required. However the cloud resolving model may be giving an incorrect estimate. Different downdraught structures might be simulated in cases of directional shear. Such sensitivities require further investigation.

The question of up-gradient transports has been commented upon. With an increase in the magnitude of the pressure gradient term, the scheme was in part able to represent some of the characteristics of the up-gradient transports associated with tropical squall lines. Although the nature of the incloud flow predicted by the parametrization was poor compared to that diagnosed from the cloud model, the results here suggest that such a mass flux approach might be able to represent such systems if the cloud model within the parametrization was more appropriate. This requires further study. However this is only part of the problem in developing a parametrization of momentum transports for organized convective systems for use within a GCM. One also has to determine when such systems might occur. This too requires further study. Several authors have suggested that convective flow regimes might be classified on the basis of a bulk Richardson number, measuring the importance of buoyant and shear effects (Moncrieff and Miller, 1976). However, observations show that a wide degree of scatter exists for different types of convection (for example see Keenan and Carbone, 1992) which suggests that using such a method may not be practical. Also, current

large-scale models lack the horizontal resolution to capture the mesoscale organization of the cloud environment which is often important for the development of organized convective systems.

The importance of the differing momentum transport associated with organised convective systems to the global circulation is as yet unknown. Indeed the transports reported above for the squall line simulation would act to increase wind errors in the tropics as simulated by the Hadley Centre Climate Model, enhancing the upper level flow. It is interesting to note that in an analysis of the momentum budget for GATE easterly waves, Zhang and Cho (1991b) show that in the presence of a low level jet similar to the tropical case simulated here convective momentum transports are downgradient. Studies of convection over the west Pacific warm pool during TOGA COARE showed extensive periods when the vertical wind shear was weak and convection relatively unorganised (Johnson, 1994). Momentum transports during such periods were presumably downgradient. These periods were interspersed by westerly wind bursts, where the usual low level easterly flow was replaced by westerly flow with strong vertical shear. Convection during these periods was more vigorous and organised into superclusters. Moncrieff and Klinker (1995) suggest that the momentum transport associated with this type of system acts to increase the vertical shear between the mid- and upper troposphere.

The parametrization developed here improves the mean circulation of the Hadley Centre Climate Model, especially in the tropics, the impact of convective momentum transports being similar to those described by Zhang and McFarlane (1995) for the Canadian Climate Centre model. The fact that the model climate is improved with the inclusion of downgradient transports suggests that the effects of unorganised convective systems dominate globally. However caution must be expressed over such an argument as errors in other parts of the model may be contributing to model systematic errors or compensating for deficiencies in the convective momentum transport parametrization.

As well as impacting upon the mean flow simulated by GCMs, the study of Slingo et al (1994) suggests the ability of GCMs to capture atmospheric variability (especially in the tropics) is very sensitive to the convection scheme used. The downgradient momentum

transports introduced into the model here will act to reduce the kinetic energy of the large-scale flow, which might be thought to act to damp variability. However this appears to be too simplistic a view. Figure 25 compares the variance of outgoing longwave radiation (OLR) on synoptic timescale (between 2 to 10 days) for the tropics of simulation C and M discussed in section 5 (3 year means). Model variability of these timescale is not always reduced. Over Africa, the tropical Atlantic and east Pacific, and also in the south Pacific convergence zone (SPCZ), the variance of OLR is clearly reduced with the introduction of convective momentum transports. Over the west Pacific and Indian Ocean it is seen to increase. The ITCZ in the central Pacific is also better defined as a distinct maximum in variance at 10N when convective momentum transports are included.

These changes may be related to the different types of synoptic systems which occur at different locations and how they are affected by the weakening of vertical shear. Easterly waves form over Africa through a mixture of baroclinic and barotropic instability on the low level easterly jet (for a recent analysis see Thorncroft, 1995). Weakening of the jet strength and vertical shear (through downgradient convective momentum transports - not shown) may result in reduced easterly wave activity. Tropical squall lines are commonly observed in the trough region of such systems. The upgradient transport of momentum associated with such systems, maintaining the strength of the low level jet, may be important in this instance. Although the HCCM has insufficient resolution to simulate tropical cyclones, depression systems are found in simulations in the west Pacific which mimic their motion. Weak vertical shear favours the formation of tropical cyclones, and so weaker shear over the west Pacific due to the inclusion of convective momentum transports (not shown) may favour the formation of more tropical depressions leading to increased variability.

These comments are speculative and confirmation of these hypotheses requires further study. However they serve to illustrate the complexity of the interaction of convective momentum transports with the large-scale flow and the continuing uncertainty over the representation of this process in large-scale models. With the increasing ability of cloud resolving models to accurately simulate convective systems in a wide variety of cases it is to be hoped that these uncertainties will be reduced over the next few years through studies such as that here.

8. REFERENCES

Brown, P.R.A. and Swann, H., 1995 : The observational validation of a 3-D numerical cloud model used for development of convective cloud parametrization schemes., Submitted to Q. J. R. Meteorol. Soc.

Browning,K.A., 1994 : GEWEX Cloud System Study (GCSS): Science Plan., World Climate Research Programme, International GEWEX Project Office, IGPO Publication Series No. 11

Cullen, M.J.P., 1993 : The Unified Forecast/Climate Model., Meteorol. Mag., **122**, 81-94

Cullen, M.J.P. and Davies, T., 1991 : A conservative split-explicit integration scheme with 4th order horizontal advection., Q. J. R. Meteorol. Soc., **117**, 993-1002

Dharssi, I., Kershaw, R. and Tao, W.-K., 1995 : Sensitivity of a simulated tropical squall line to longwave radiation., Submitted to Q. J. R. Meteorol. Soc.

Dolman, A.J. and Gregory, D, 1992 : The parametrization of rainfall interception in GCMs., Q. J. R. Meteorol. Soc., **118**, 455-467

Flatau, M. and Stevens, D.E., 1987 : The effect of horizontal pressure gradients on the momentum transport in tropical convective lines. II, Lagrangian calculations., J. Atmos. Sci., **44**, 2088-2096

Gregory, D., 1995 : Convection scheme. Part 2: Description of downdraught., UM Documentation Paper No. 27-2, Available from the Unified Model Librarian, NWP-Div., Meteorological Office, London Road, Bracknell, Berks. RG12 2SZ. United Kingdom

Gregory, D. and Allen, S., 1991 : The effect of convective scale downdraughts upon NWP and climate simulations., Preprints of the 9th Conf. on Numerical Weather Prediction, Oct 14-18, 1991, Denver, Co., USA

Gregory, D. and Miller, M.J., 1989 : A numerical study of the parametrization of deep tropical convection., Q. J. R. Meteorol. Soc., **115**, 1209-1241

Gregory, D. and Rowntree, P.R., 1990 : A mass flux convection scheme with representation of cloud ensemble characteristics and stability dependent closure., Mon. Wea. Rev., **118**, 1483-1506

Gregory, D., Shutts, G.J. and Mitchell, J.M., 1995 : A parametrization of gravity wave drag incorporating the anisotropic effects of orography and low level wave breaking: Performance in the Met. Office Unified Model., In preparation

Hall, C.D., Stratton, R.A. and Gallani, M.L., 1995 : Climate simulations with the Unified Model: AMIP runs., In preparation

Helfand, H.M., 1979 : The effect of cumulus friction on the simulation of the January Hadley circulation by the GLAS model of the general circulation., J. Atmos. Sci., **36**, 1827-1843

Ingram, W.J., 1993 : Radiation., Unified Model Documentation Paper No. 23, Available from the Unified Model Librarian, NWP-Div., Meteorological Office, London Road, Bracknell, Berks. RG12 2SZ. United Kingdom

Johnson, R.H., 1994 : Observations for validating cumulus parametrizations., ECMWF Seminar proceedings on "Parametrization of sub-grid scale physical processes", 5-9 Sept 1994, ECMWF, Shinfield Park, Reading, UK

Keenan, T.D. and Carbone, R.E., 1992 : A preliminary morphology of precipitation systems in tropical northern Australia., Q. J. R. Meteorol. Soc., **118**, 282-326

Kershaw, R. and Gregory, D., 1995 : Parametrization of momentum transports by convection. I: Theory and cloud modelling results., Submitted to Q. J. R. Meteorol. Soc.

König, W. and Ruprecht, E., 1989 : Effects of convective clouds on the large-scale vorticity budget., Meteorol. and Atmos. Phys., **41**, 213-229

LeMone, M.A., 1983 : Momentum transport by a line of cumulonimbus., J. Atmos. Sci., **40**, 1815-1834

Moncrieff, M.W. and Miller, M.J., 1976 : the dynamics and simulation of tropical cumulonimbus and squall lines., Q. J. R. Meteorol. Soc., **102**, 373-394

Moncrieff, M.W. and Klinker, E., 1995 : Mesoscale cloud systems in the tropical western Pacific as a process in general circulation models., Submitted to Q. J. R. Meteorol. Soc.

Nordeng, T.E., 1995 : Extended versions of the convective parametrization scheme at ECMWF and their impact upon the mean and transient activity of the model in the tropics., Submitted to Q. J. R. Meteorol. Soc.

Senior, C.A. and Mitchell, J.F.B., 1993 : Carbon Dioxide and climate: Impact of cloud parametrization., J. Climate, **6**, 393-417

Shapiro, L. and Stevens, D., 1980 : Parametrization of convective effects on the momentum and vorticity budgets of synoptic-scale Atlantic tropical waves., Mon. Wea. Rev., **108**, 1816-1826

Slingo, A., 1989 : A GCM parametrization for the shortwave radiative properties of water cloud., J. Atmos. Sci., **46**, 1419-1427

Slingo, J., Blackburn, M., Betts, A., Brugge, R., Hodges, K., Hoskins, B., Miller, M., Steenman-Clark, L. and Thuburn, J., 1994 : Mean climate and transience in the tropics of the UGAMP GCM: Sensitivity to convective parametrization., Q. J. R. Meteorol. Soc., **120**, 881-922

Smith, R.N.B., 1990 : A scheme for predicting layer clouds and their water contents in a general circulation model., Q. J. R. Meteorol. Soc., **116**, 435-460

Smith, R.N.B., 1994 : Experience and developments with layer cloud and boundary layer mixing scheme in the UKMO Unified Model., ECMWF Workshop on the "Parametrization of the cloud topped boundary layer", 8-11 June 1993, Shinfield Park, Reading, Berks.

Smith, R.N.B., Jackson, S. and Milton, S.F., 1995 : A parametrization of orographic form drag and its effects in the UK Meteorological Office Unified Model., In preparation

Thorncroft, C.D., 1985 : An idealised study of African easterly waves. III: More realistic basic states., Q. J. R. Meteorol. Soc., **121**, 1589-1614

Tiedtke, M., 1989 : A comprehensive mass flux scheme for cumulus parametrization in large-scale models., Mon. Wea. Rev., **117**, 1779-1800

Warrilow, D.A., Sangster, A.B. and Slingo, A., 1986 : Modelling of land surface processes and their influence on European climate., Dynamical Climatology Technical Note No. 38, Available from the Hadley Centre, Meteorological Office, London Road, Bracknell, Berks. RG12 2SY. United Kingdom

Zhang, G.J. and Cho, H-R., 1991a : Parametrization of the vertical transport of momentum by cumulus clouds. Part I: theory., J. Atmos. Sci., **48**, 1483-1492

Zhang, G.J. and Cho, H-R., 1991b : Parametrization of the vertical transport of momentum by cumulus clouds. Part II: application., J. Atmos. Sci., **48**, 2448-2457

Zhang, G.J. and McFarlane, N.A., 1995 : Role of convective scale momentum transport in climate simulation., J. Geophys. Res., **100**, 1417-1426

List of Figures

Figure 1a Vertical discretisation of updraught in the parametrization scheme.

Figure 1b Vertical discretisation of downdraught in the parametrization scheme.

Figure 2 Comparison of vertical profiles of updraught (UD) and downdraught (DD) mass flux from the cloud resolving model (experiment 232 - UD : solid, DD : dashed) and the parametrization scheme (experiment S32ncpg - UD : long dash, DD : dot-dash) for a cold air outbreak case. 10 hour averages.

Figure 3 Comparison of horizontal velocity within (a) the updraught (UD) and (b) the downdraught with the large-scale velocity (LSU) for the cloud resolving model (experiment 232 - LSU : solid, UD/DD : dashed) and parametrization (experiment S32ncpg - LSU : long dashed, UD/DD : dot-dash) for a cold air out break case. 10 hour averages.

Figure 4 Vertical eddy momentum flux due to (a) updraught and downdraught for cloud resolving model (experiment 232 - UD : solid, DD : dashed) and parametrization scheme (experiment S32ncpg - UD : long dash, DD : dot-dash) and (b) whole cloud for cloud resolving model (experiment 232) : solid and parametrization scheme (experiment S32ncpg) : long dash for a cold air out break. 10 hour averages

Figure 5 Comparison of effect of vertical pressure gradient upon horizontal velocity within cloud updraughts diagnosed from experiments with the cloud resolving model for a variety of wind shears and surface fluxes. Experiment 232 : Solid, 233 : dashed, 236 : long dash and 237 : dot-dash). 10 hour averages.

Figure 6 Comparison of parametrized pressure gradient term with that diagnosed from the cloud resolving model simulations for updraughts and downdraughts. Experiment 232 - UD : Solid, DD : dashed. Experiment S32 - UD : long dash, DD : dot-dash). 10 hour averages.

Figure 7 As figure 3 but for experiments 232 and S32.

Figure 8 Q3 diagnosed from cloud resolving model experiment 232 (solid) and predicted by the parametrization scheme in experiments S32ncpg (dash) and S32 (long dash). 10 hour averages.

Figure 9 As figure 6 but for experiments 237 and S37.

Figure 10 As for figure 8 but for experiments 237 and S37.

Figure 11 Cooling (solid) and moistening (dashed) due to implied large-scale ascent applied to cloud resolving and single column model experiments for the tropical case.

Figure 12 As for figure 2 but for experiments 235 and S35 for the tropical case.

Figure 13 As for figure 6 but for experiments 235 and S35 for the tropical case.

Figure 14 Horizontal velocity within the cloud updraught (UD) compared with the large-scale value (LSU) for experiments 235 (UD : dashed, LSU : Solid) and experiment S35 - (UD : dot-dash, LSU : long dashed) for the tropical case. 10 hour averages.

Figure 15 As fig 8 but for experiments 235 (solid), 234 (dot-dashed), S35ncpg (dashed) and S35 (long dash).

Figure 16 Pressure gradient term for the updraught as diagnosed from experiments 235 (solid) and 234 (long dashed) together with that predicted by the parametrization for experiments S34 (dashed). 10 hour averages.

Figure 17 As for figure 14 but for experiments 234 and S34.

Figure 18 Vertical eddy momentum flux due to updraughts : Cloud resolving model (experiment 234) : solid, parametrization scheme (experiment S34) : dash). 10 hour averages.

Figure 19 Contribution to the acceleration of the zonal mean flow by (a)dynamics, (b)boundary layer and (c) gravity wave drag for DJF (3 year mean) for simulation C (without convective momentum transports).

Figure 20 Contribution to the acceleration of the zonal mean flow by (a)dynamics, (b)boundary layer, (c) gravity wave drag and (d)convection for DJF (3 year mean) for simulation M.

Figure 21 Contribution to the acceleration of the meridional flow due to convection for DJF (3 year mean) for simulation M.

Figure 22 Height-latitude cross-section of zonal mean wind estimated from (a) ECMWF analyses between 1985 and 1993 for DJF together with differences of wind field predicted by (b) simulation C and (c) M (3 year means) from the ECMWF data.

Figure 23 Height-latitude cross-section of zonal mean meridional wind estimated from (a) ECMWF analyses between 1985 and 1993 for DJF together with that predicted by (b) simulations C and (c) M (3 year means).

Figure 24 Height-latitude cross-section of zonal mean wind estimated from (a) ECMWF analyses between 1985 and 1993 for JJA together with differences of wind field predicted by (a) simulation C and (c) simulation M (3 year means).

Figure 25 Variance of outgoing longwave radiation $((Wm^{-2})^2)$ in the tropics on synoptic timescale (between 2 and 10 days) for (a) simulation C and (b) simulation M (3 year mean).

List of tables

Table 1 List of cold-air outbreak experiments.

Table 2 List of tropical experiments.

Single Column Model Experiment	Parallel Cloud Resolving Model Experiment (as in KG95)	Shear (m/s/6km)	Surface latent heat flux (W/m^2)	Surface sensible heat flux (W/m^2)
S32npg	232	10	400	100
S32	232	10	400	100
S33	233	20	400	100
S36	236	10	800	100
S37	237	20	800	100

Table 1 List of cold-air outbreak experiments.

Single Column Model Experiment	Parallel Cloud Resolving Model Experiment (as in KG95)	Surface latent heat flux (W/m^2)	Surface sensible heat flux (W/m^2)	Coefficient in parametrization of cloud pressure gradient
S35npg	235 (3D)	125	25	0
S35	235 (3D)	125	25	0.7
S34	234 (2D)	125	25	1.4

Table 2 List of tropical experiments.

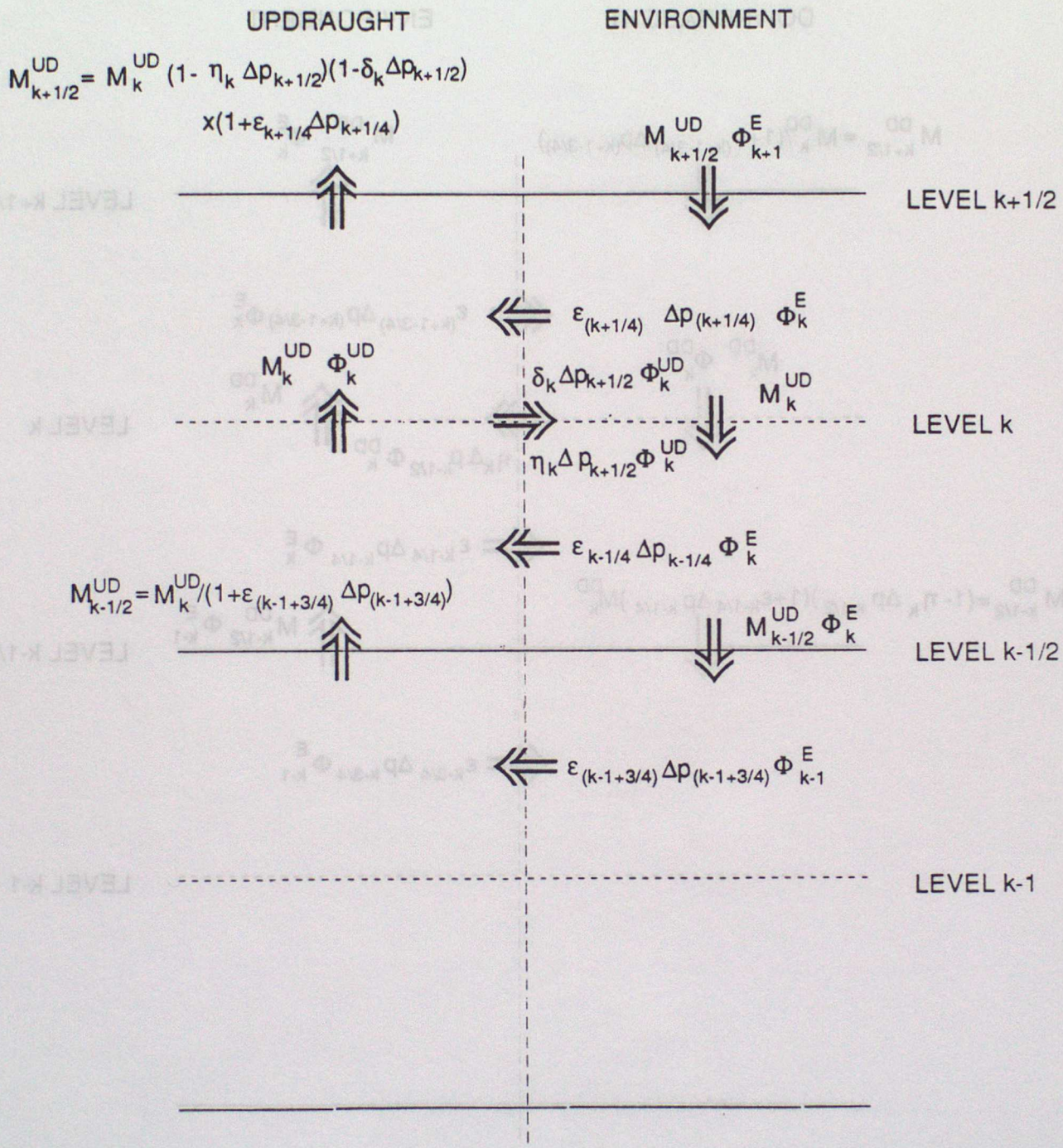
UPDRAUGHT
ENVIRONMENT
$M^{UD}_{k+1/2} = M^{UD}_{k} (1 - \eta_k \Delta p_{k+1/2})(1 - \delta_k \Delta p_{k+1/2})$
$x(1 + \varepsilon_{k+1/4} \Delta p_{k+1/4})$
$M^{UD}_{k+1/2}\ \Phi^{E}_{k+1}$
LEVEL k+1/2
$\varepsilon_{(k+1/4)}\ \Delta p_{(k+1/4)}\ \Phi^{E}_{k}$
$M^{UD}_{k}\ \Phi^{UD}_{k}$
$\delta_k \Delta p_{k+1/2}\ \Phi^{UD}_{k}$
M^{UD}_{k}
LEVEL k
$\eta_k \Delta p_{k+1/2} \Phi^{UD}_{k}$
$\varepsilon_{k-1/4}\ \Delta p_{k-1/4}\ \Phi^{E}_{k}$
$M^{UD}_{k-1/2} = M^{UD}_{k} / (1 + \varepsilon_{(k-1+3/4)}\ \Delta p_{(k-1+3/4)})$
$M^{UD}_{k-1/2}\ \Phi^{E}_{k}$
LEVEL k-1/2
$\varepsilon_{(k-1+3/4)}\ \Delta p_{(k-1+3/4)}\ \Phi^{E}_{k-1}$
LEVEL k-1

Figure 1a

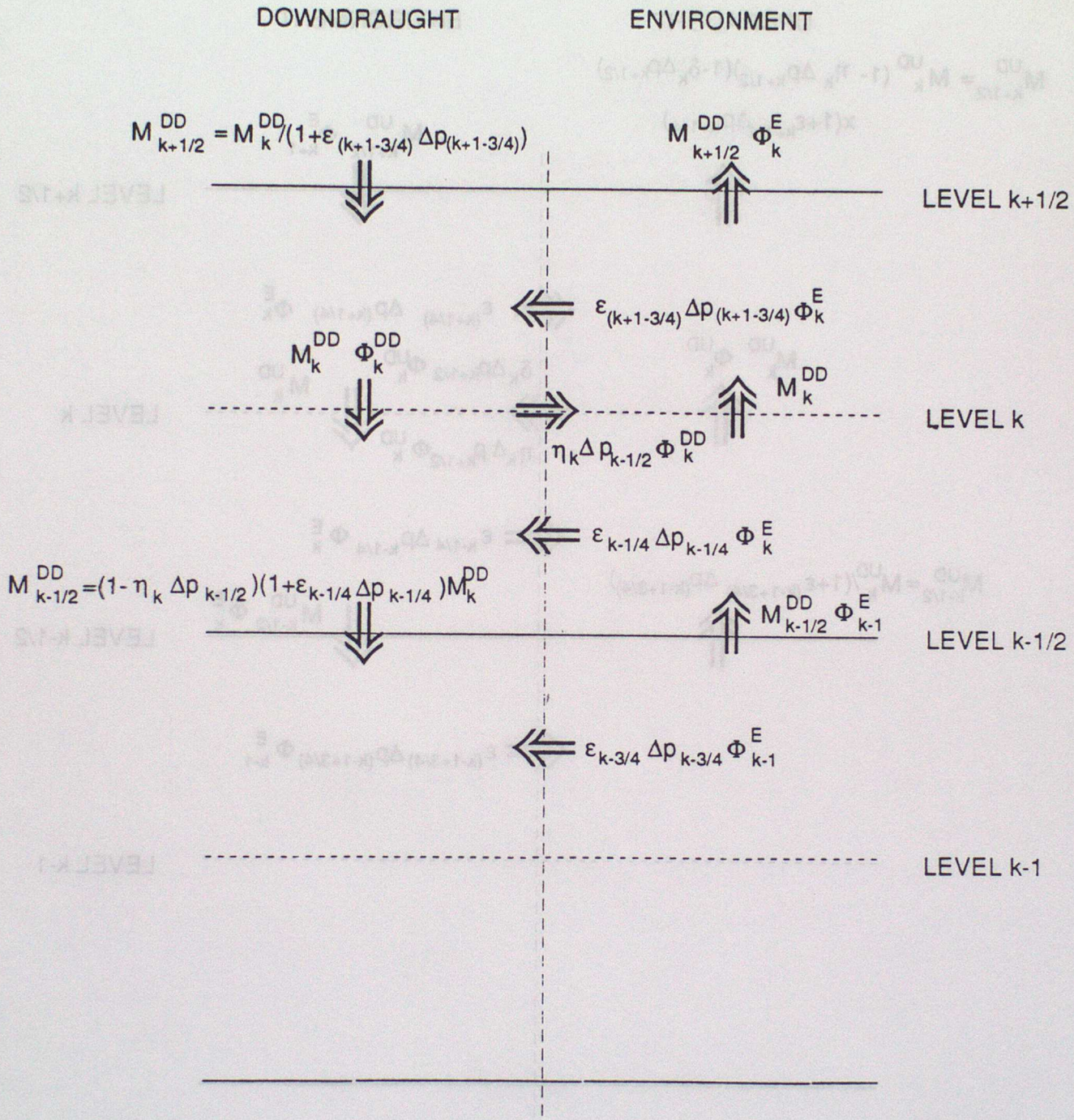
DOWNDRAUGHT
ENVIRONMENT
$M^{DD}_{k+1/2} = M^{DD}_{k}/(1+\varepsilon_{(k+1-3/4)}\,\Delta p_{(k+1-3/4)})$
$M^{DD}_{k+1/2}\,\Phi^{E}_{k}$
LEVEL k+1/2
$\varepsilon_{(k+1-3/4)}\,\Delta p_{(k+1-3/4)}\,\Phi^{E}_{k}$
$M^{DD}_{k}\;\Phi^{DD}_{k}$
M^{DD}_{k}
LEVEL k
$\eta_k \Delta p_{k-1/2}\,\Phi^{DD}_{k}$
$\varepsilon_{k-1/4}\,\Delta p_{k-1/4}\,\Phi^{E}_{k}$
$M^{DD}_{k-1/2}=(1-\eta_k\,\Delta p_{k-1/2})(1+\varepsilon_{k-1/4}\,\Delta p_{k-1/4})M^{DD}_{k}$
$M^{DD}_{k-1/2}\,\Phi^{E}_{k-1}$
LEVEL k-1/2
$\varepsilon_{k-3/4}\,\Delta p_{k-3/4}\,\Phi^{E}_{k-1}$
LEVEL k-1

Figure 1b

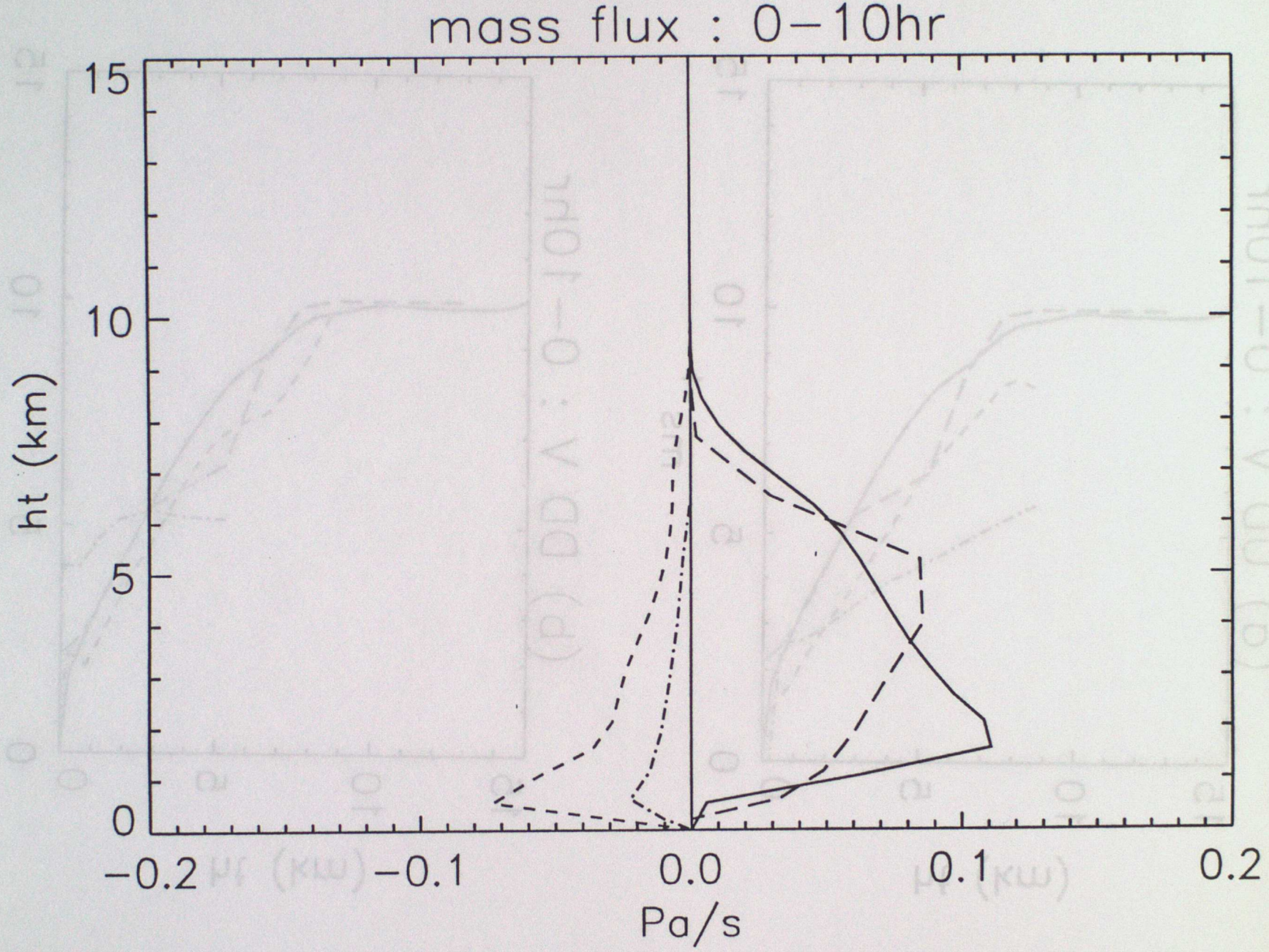

Figure 2

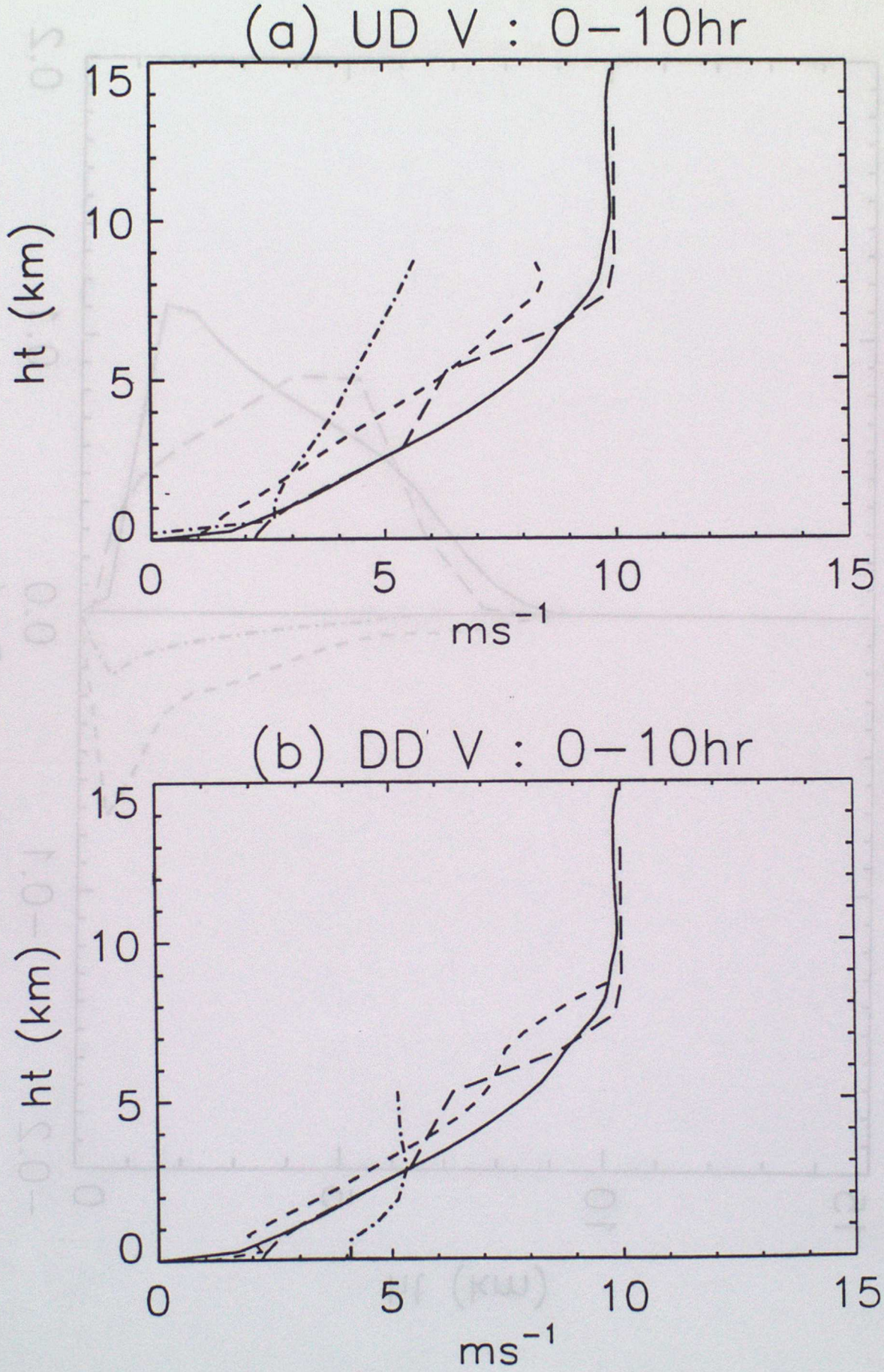
(a) UD V : 0–10hr
ht (km)
15
10
5
0
0
5
10
15
ms^{-1}
(b) DD V : 0–10hr
ht (km)
15
10
5
0
0
5
10
15
ms^{-1}

Figure 3

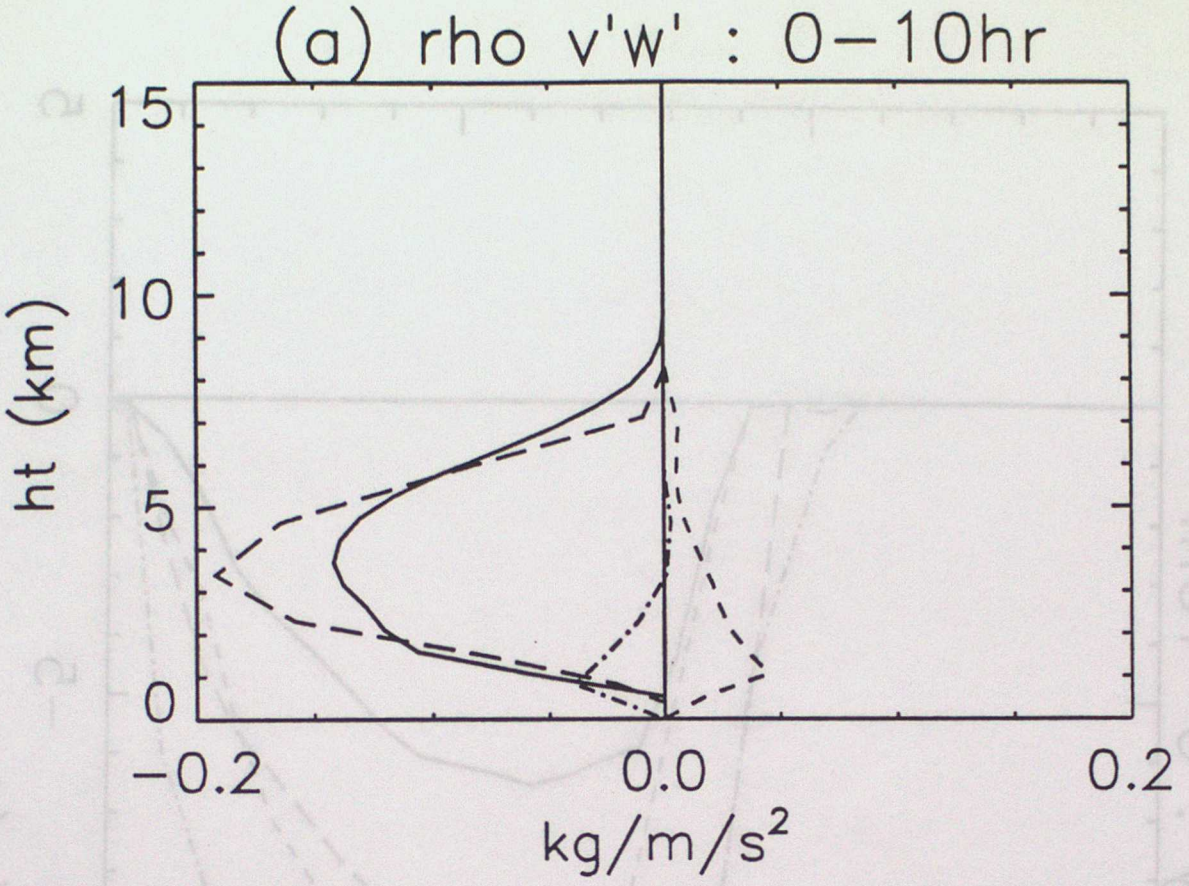
(a) rho v'w' : 0–10hr
15
10
5
0
ht (km)
−0.2
0.0
0.2
kg/m/s²

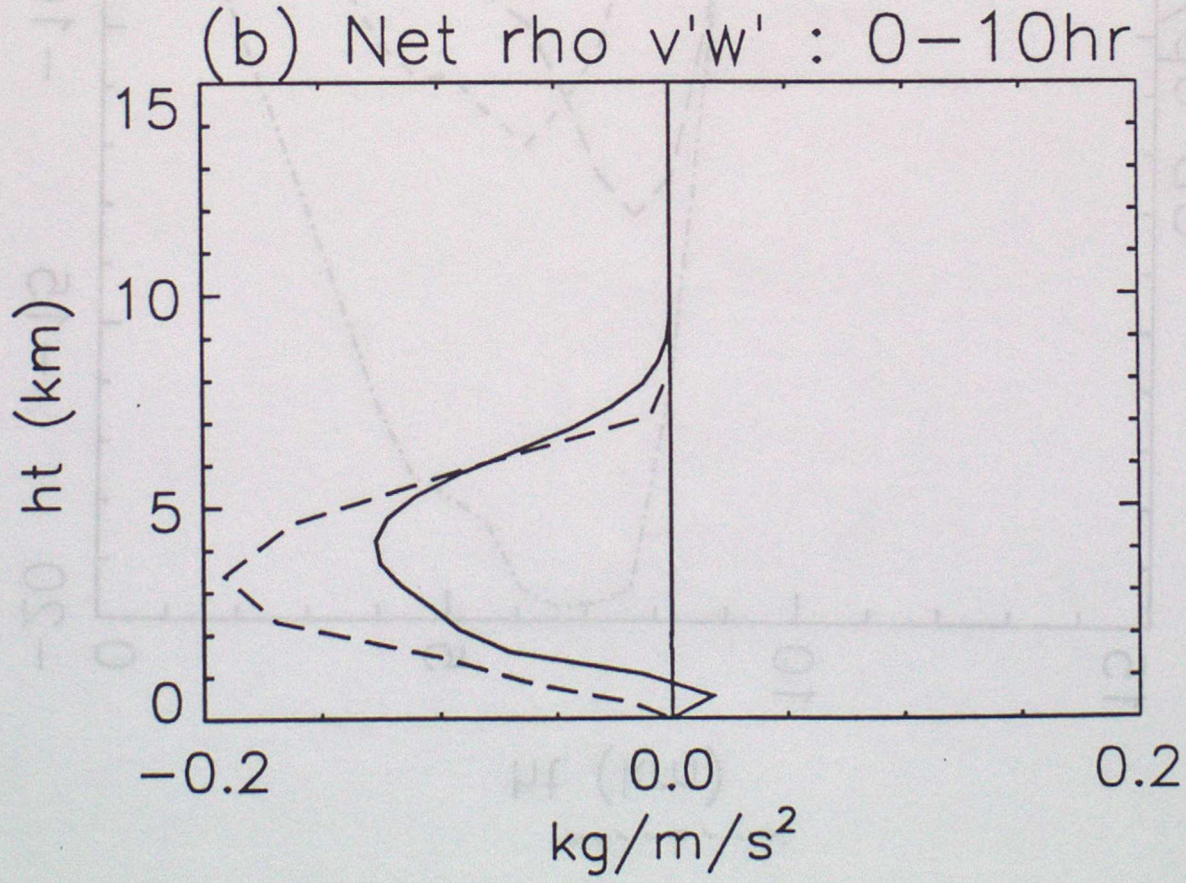
(b) Net rho v'w' : 0–10hr
15
10
5
0
ht (km)
−0.2
0.0
0.2
kg/m/s²

Figure 4

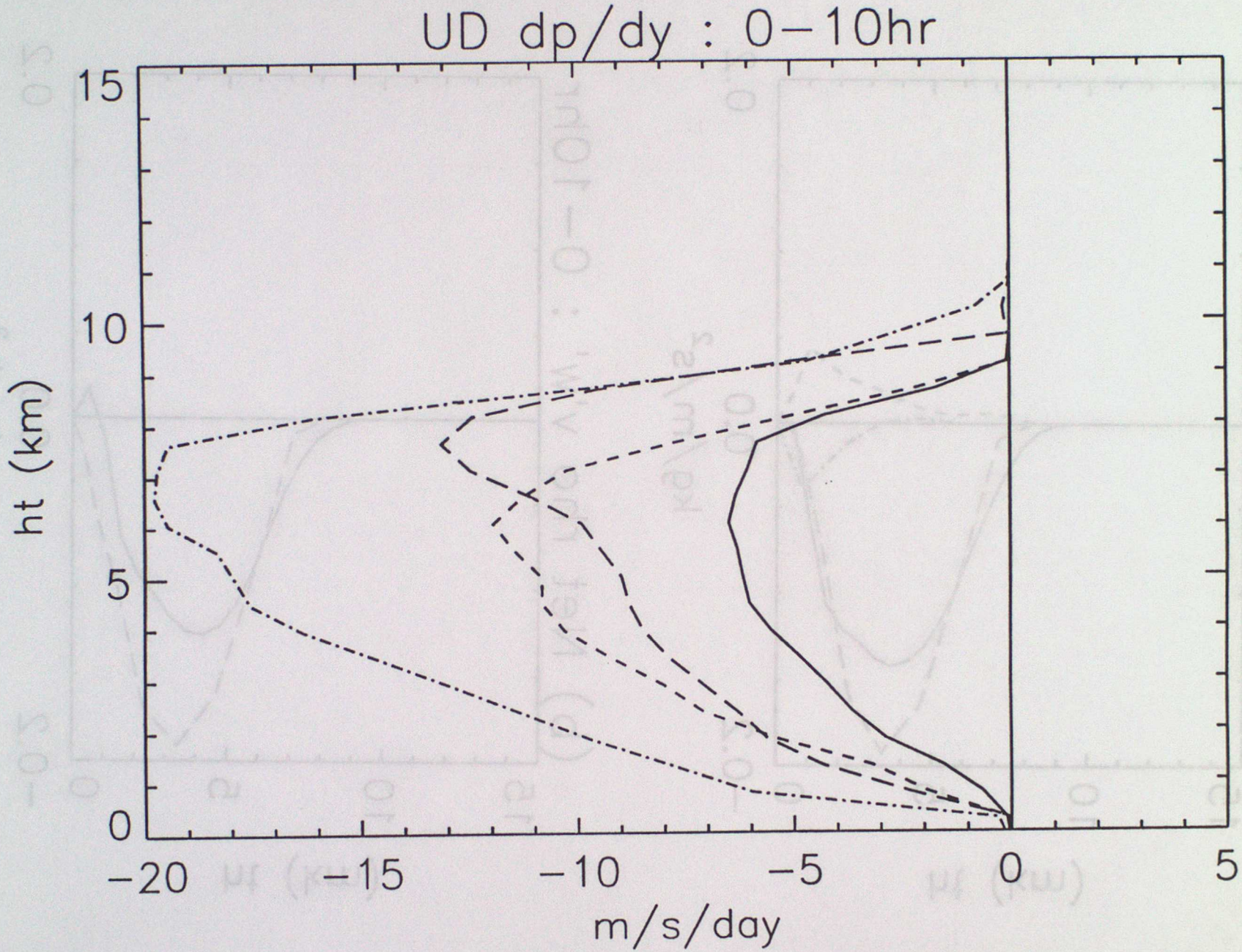

Figure 5

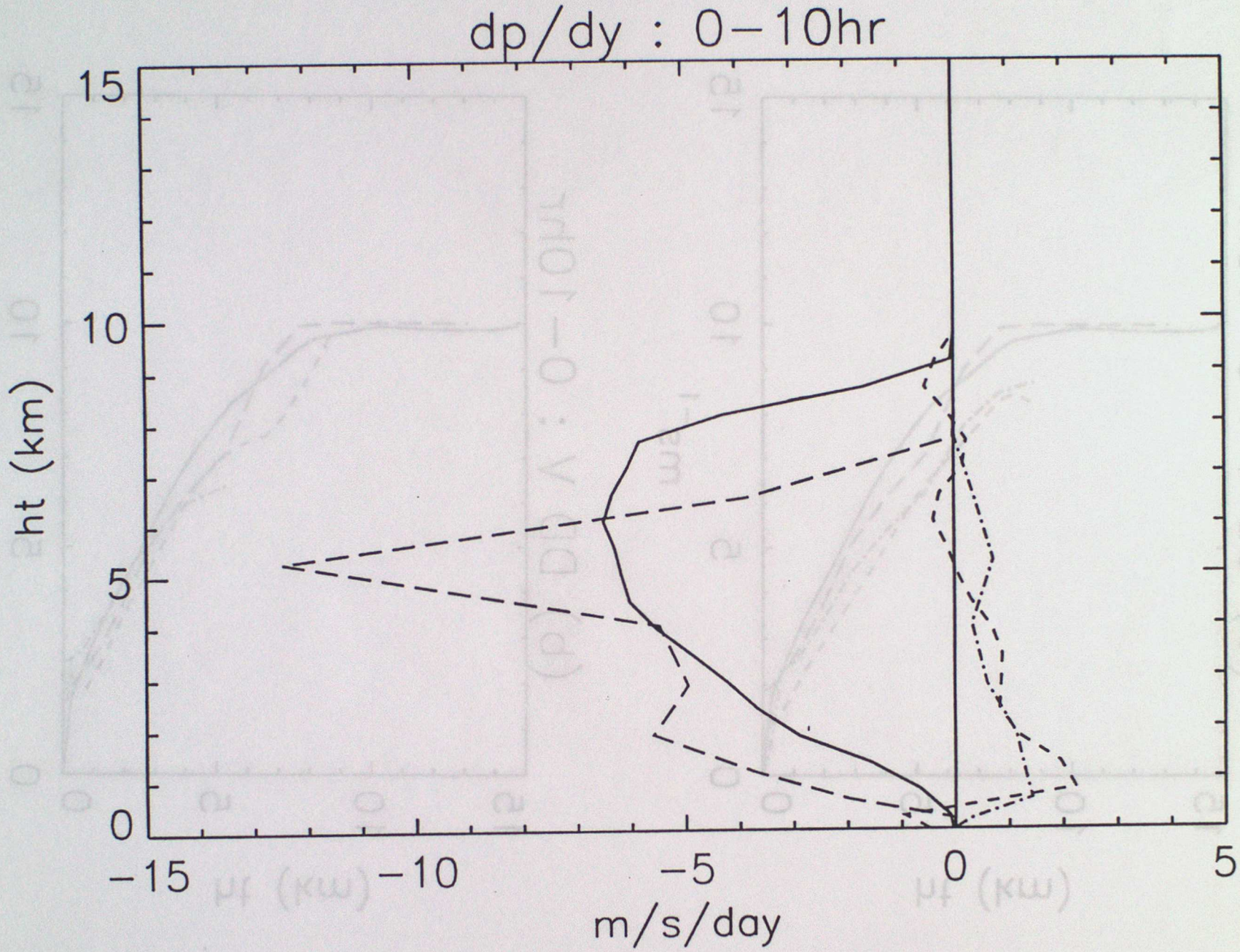

Figure 6

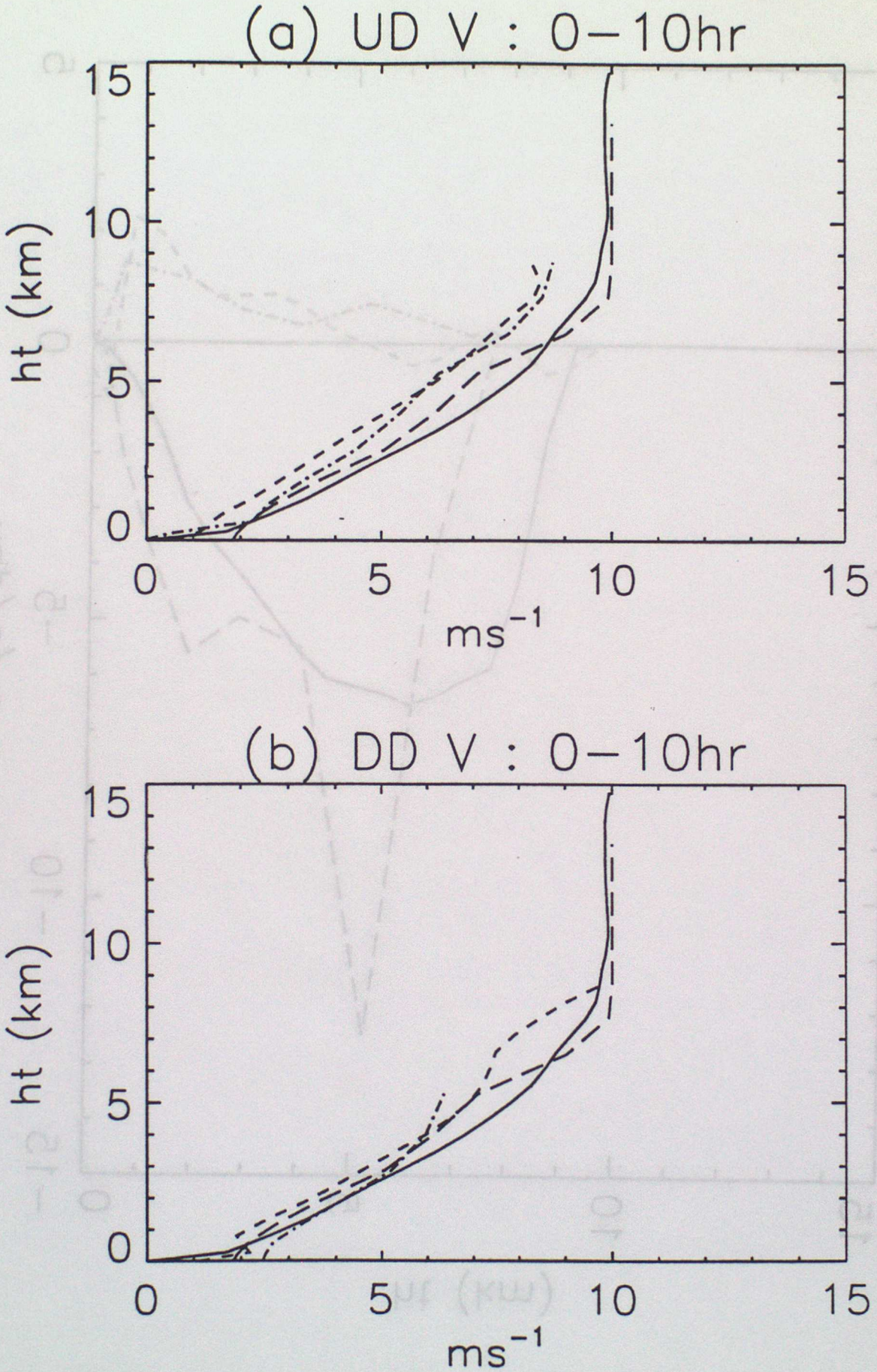
(a) UD V : 0–10hr
ht (km)
15
10
5
0
0
5
10
15
ms^{-1}
(b) DD V : 0–10hr
ht (km)
15
10
5
0
0
5
10
15
ms^{-1}

Figure 7

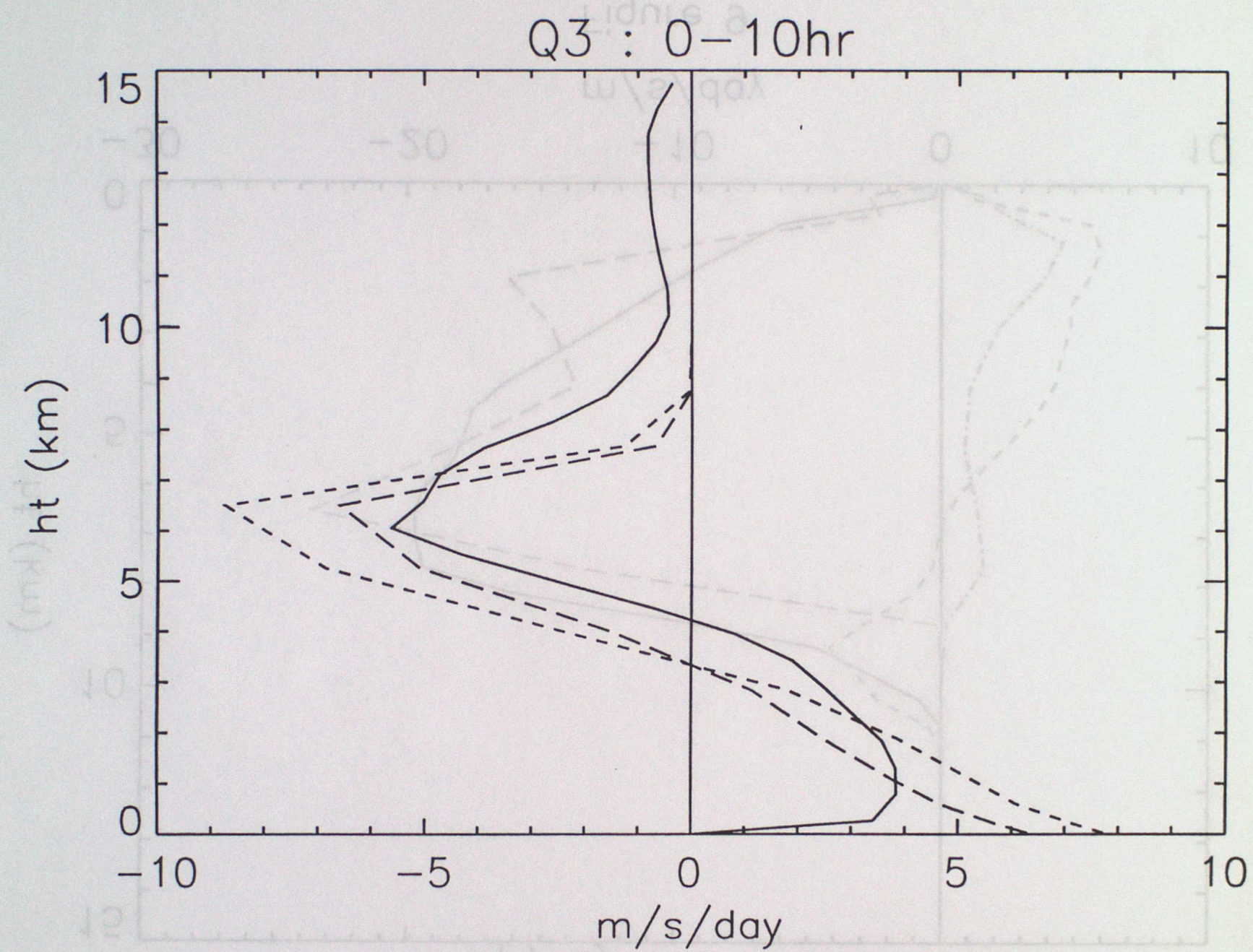

Figure 8

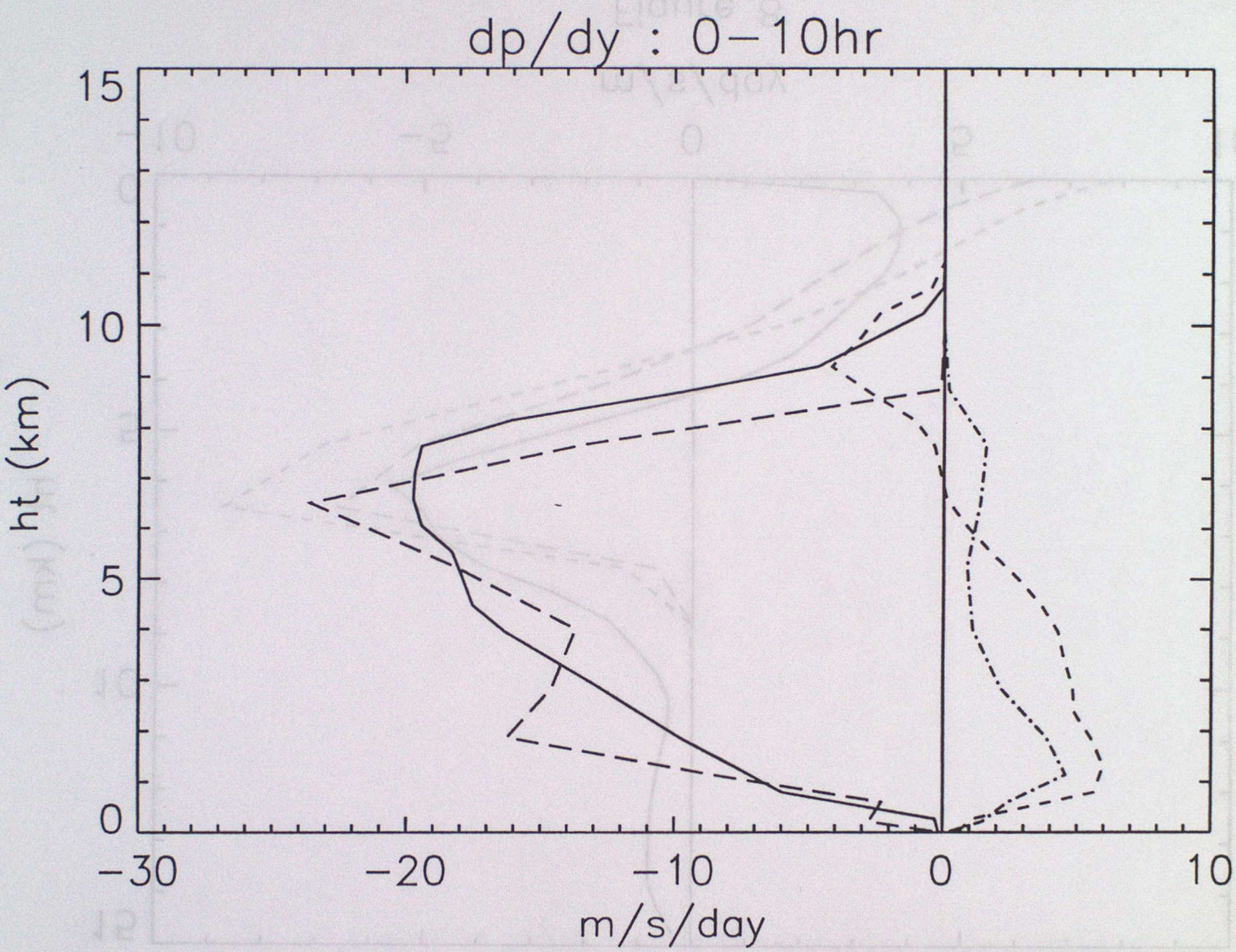

Figure 9

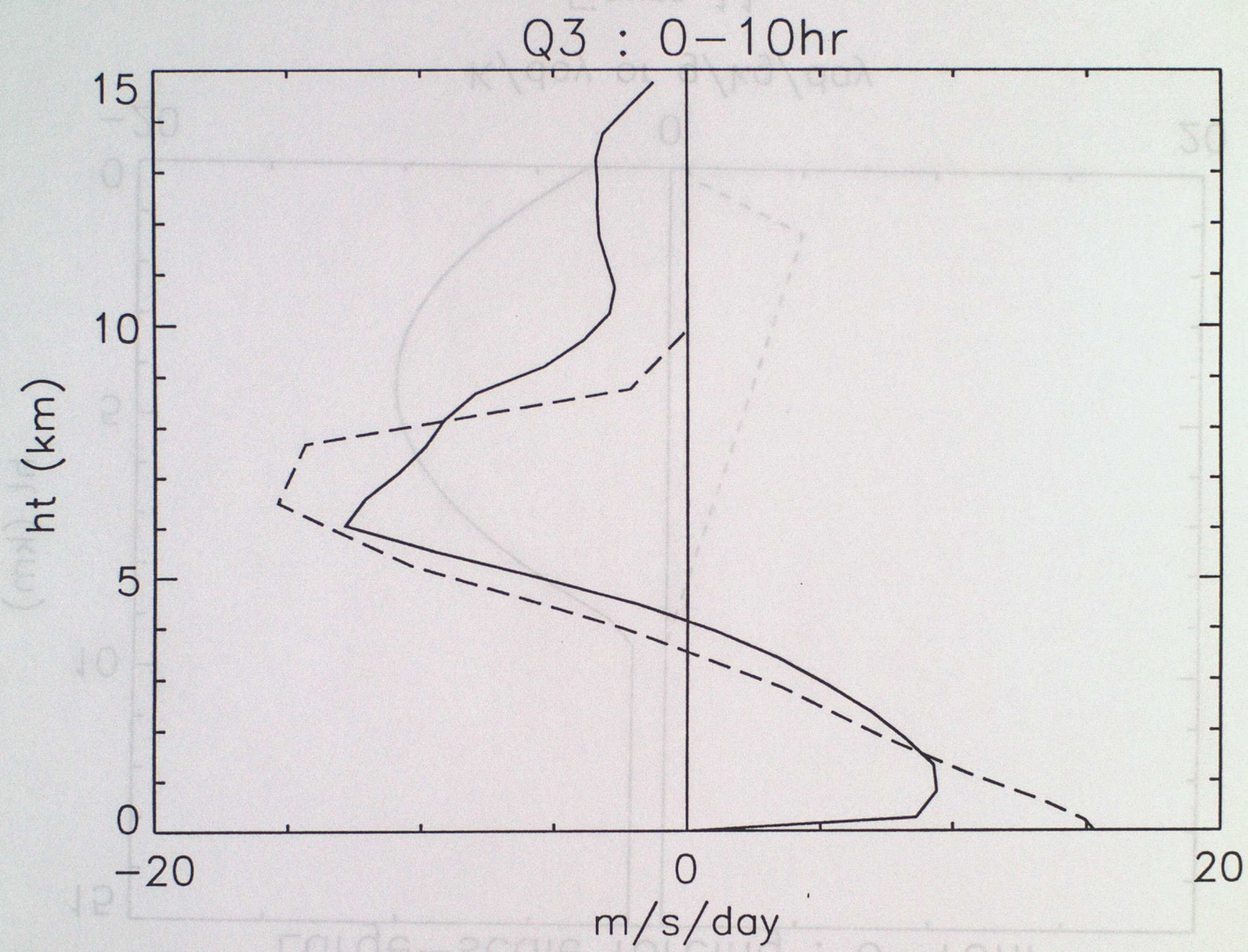

Figure 10

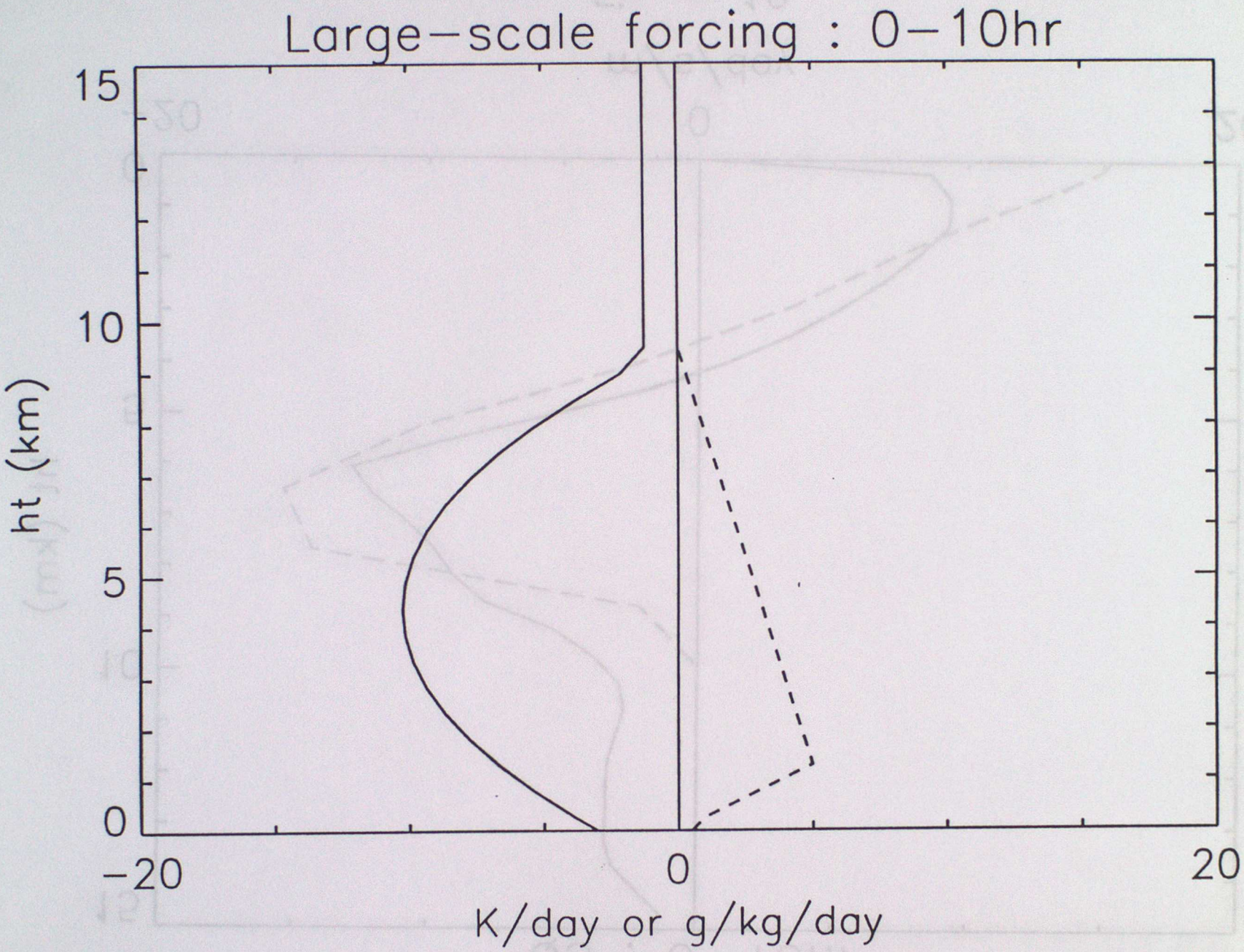

Figure 11

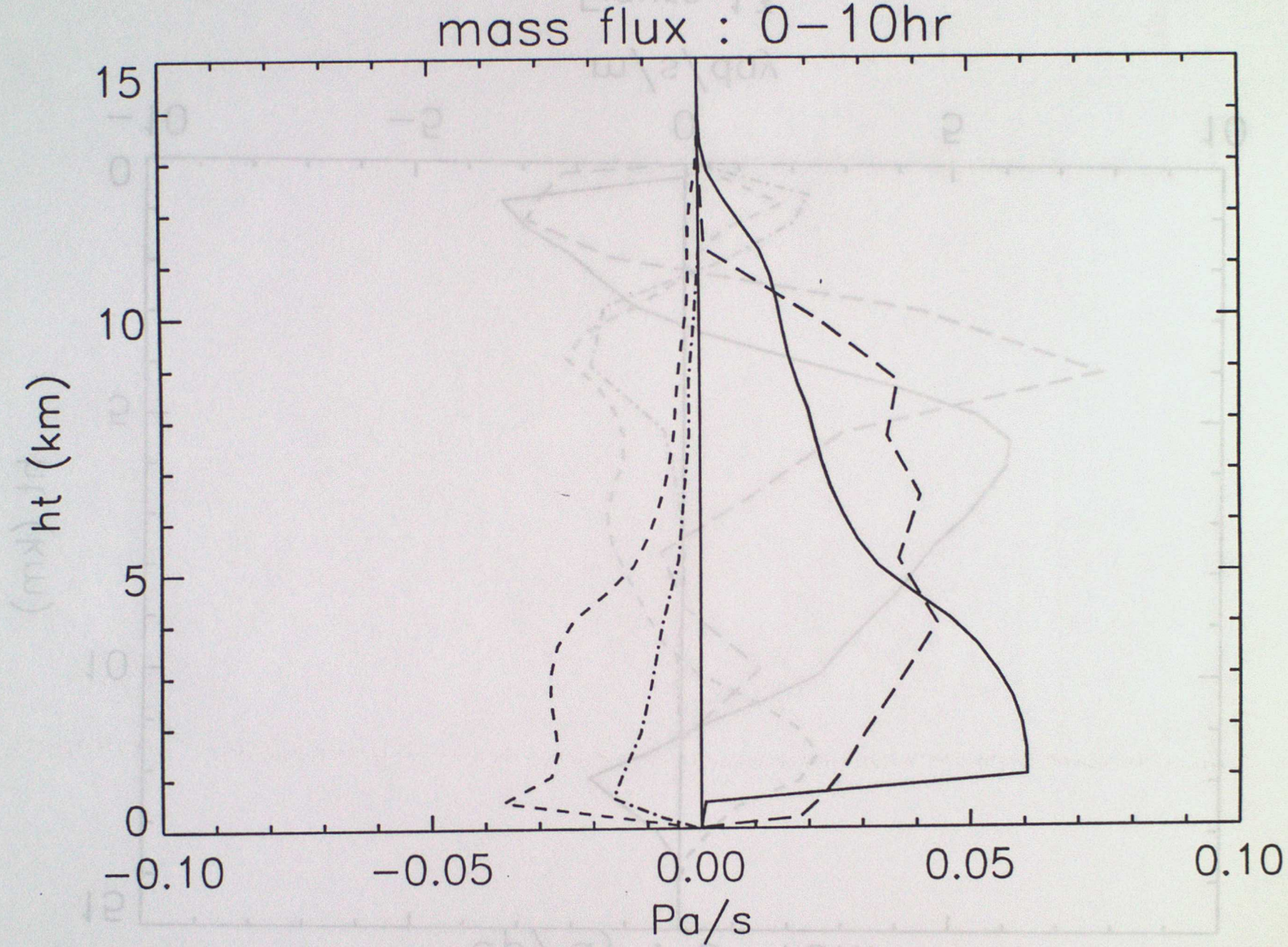

Figure 12

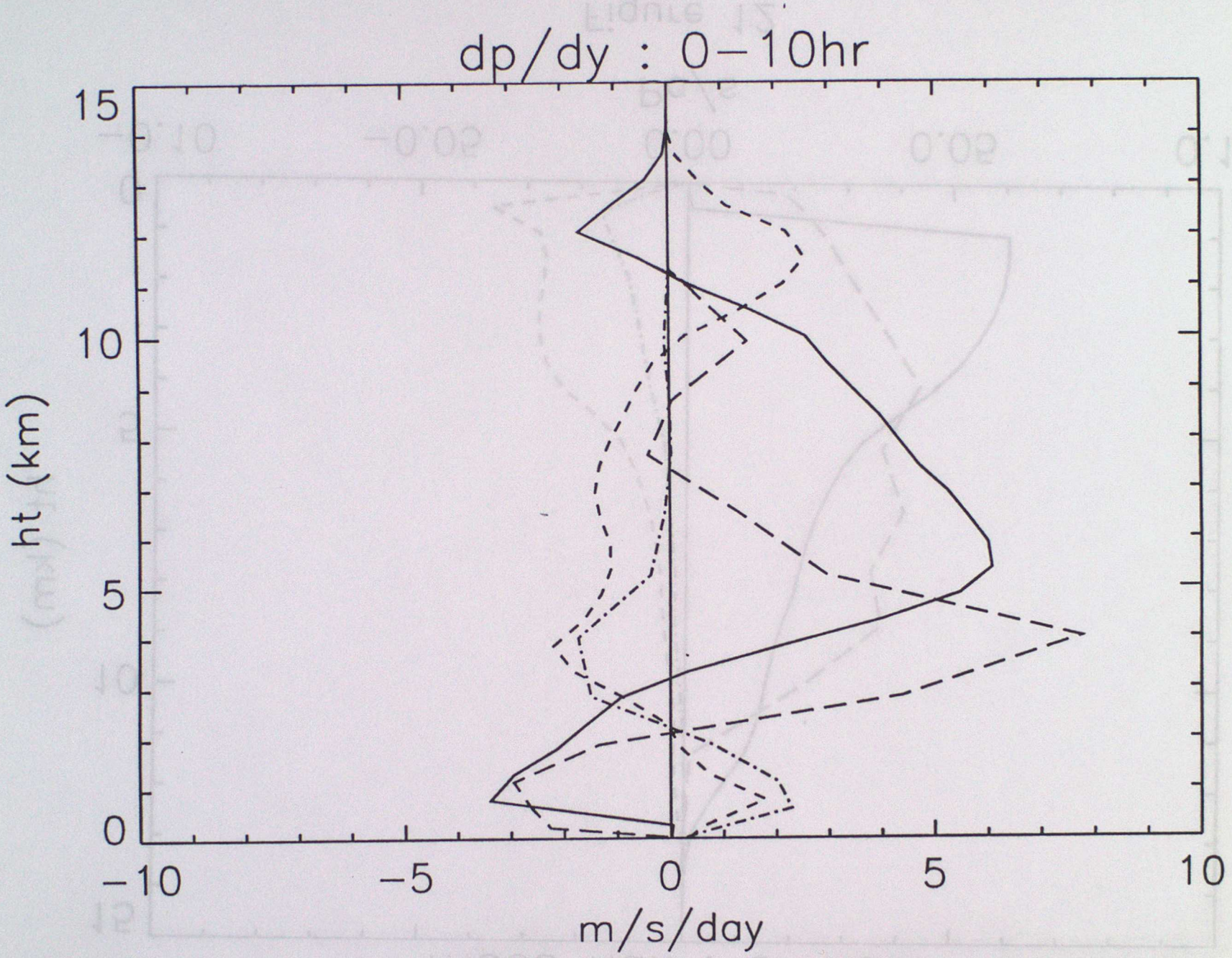

Figure 13

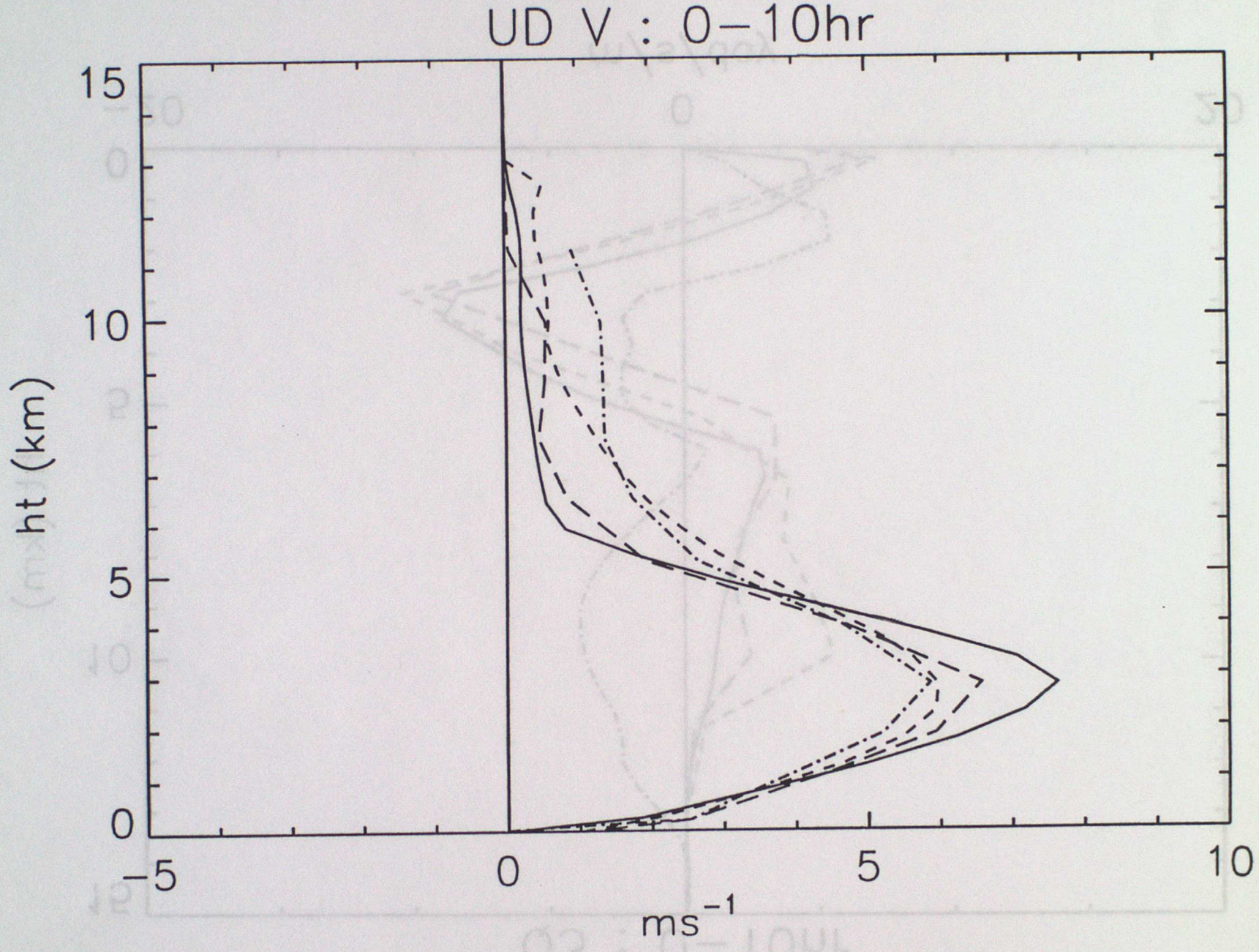

Figure 14

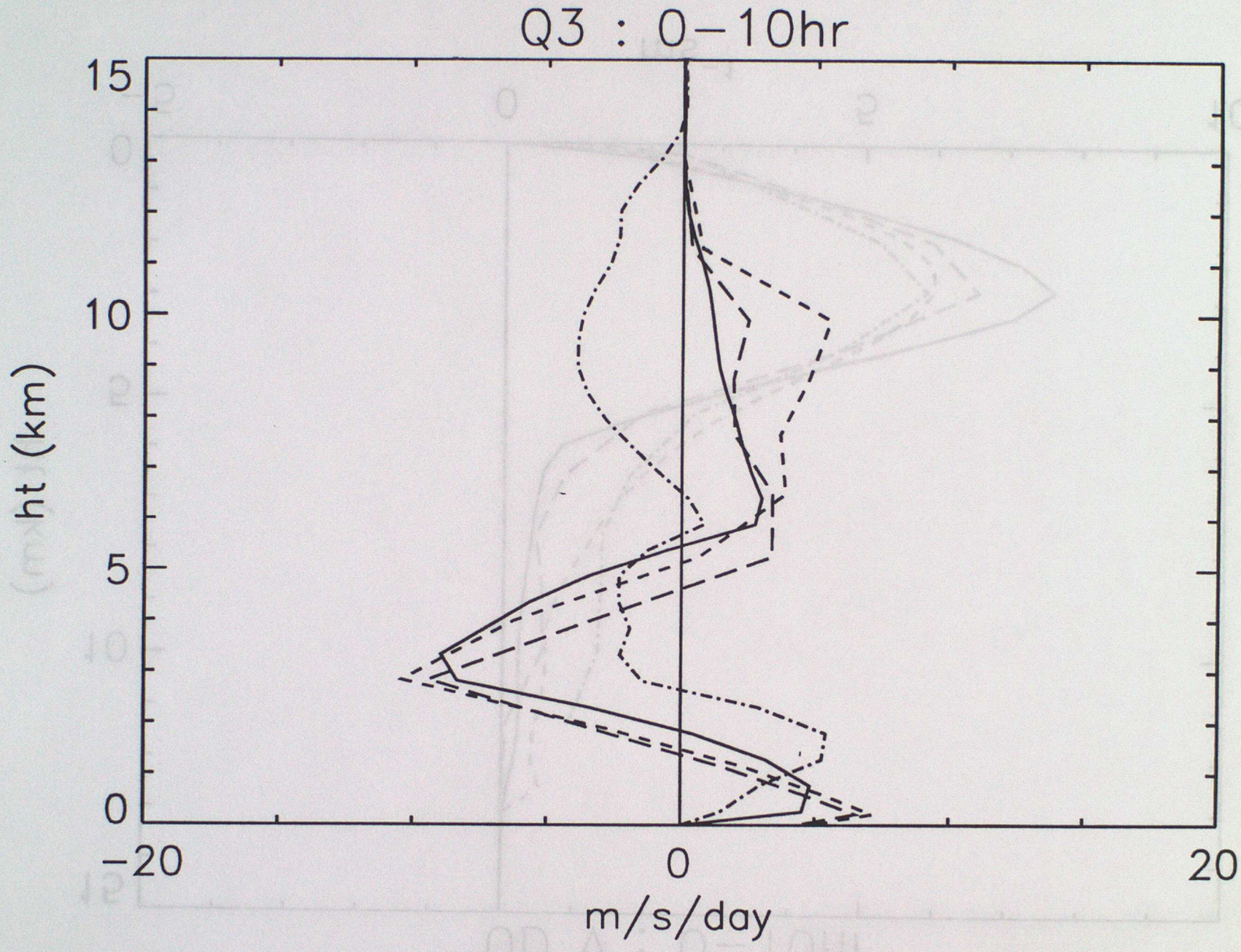

Figure 15

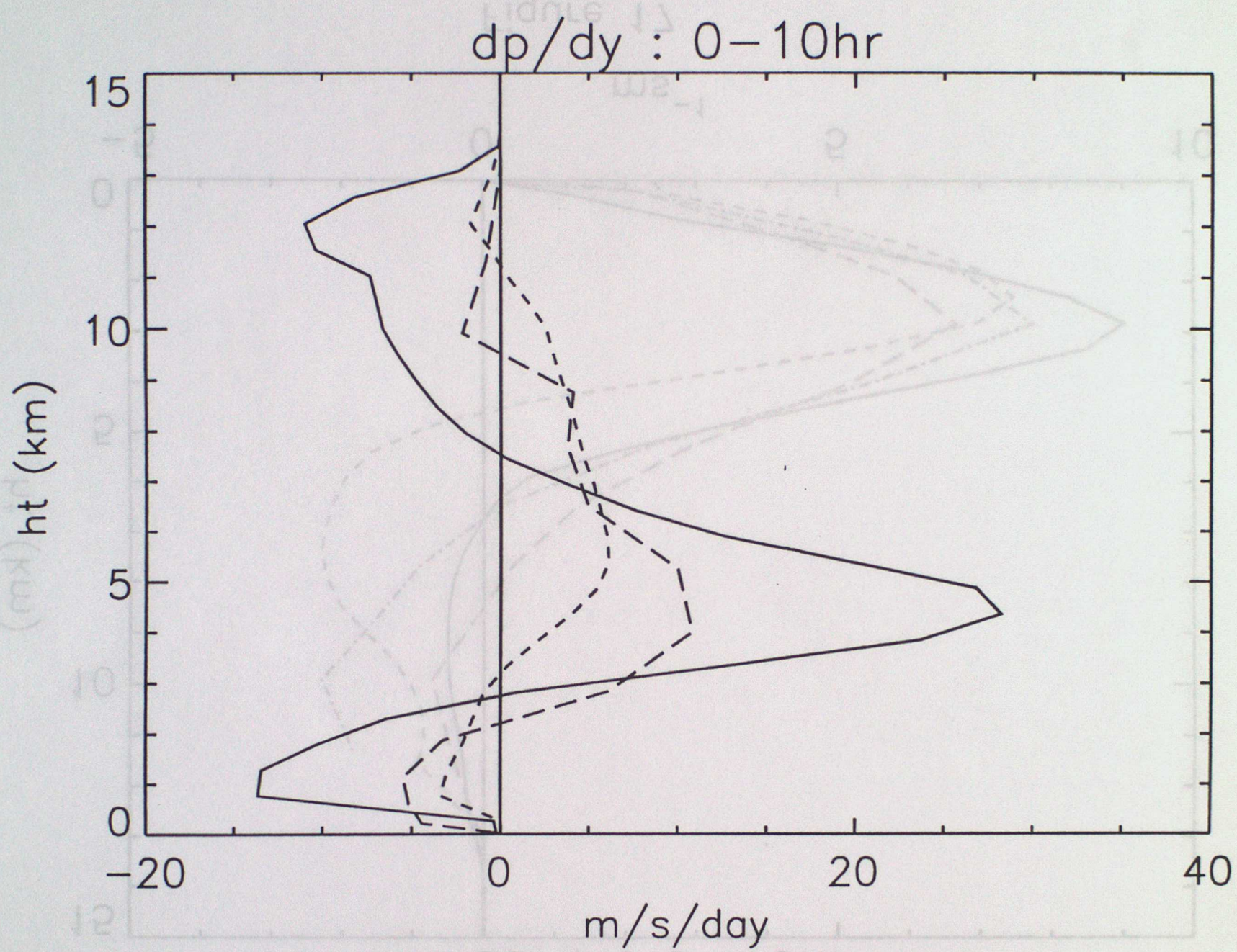

Figure 16

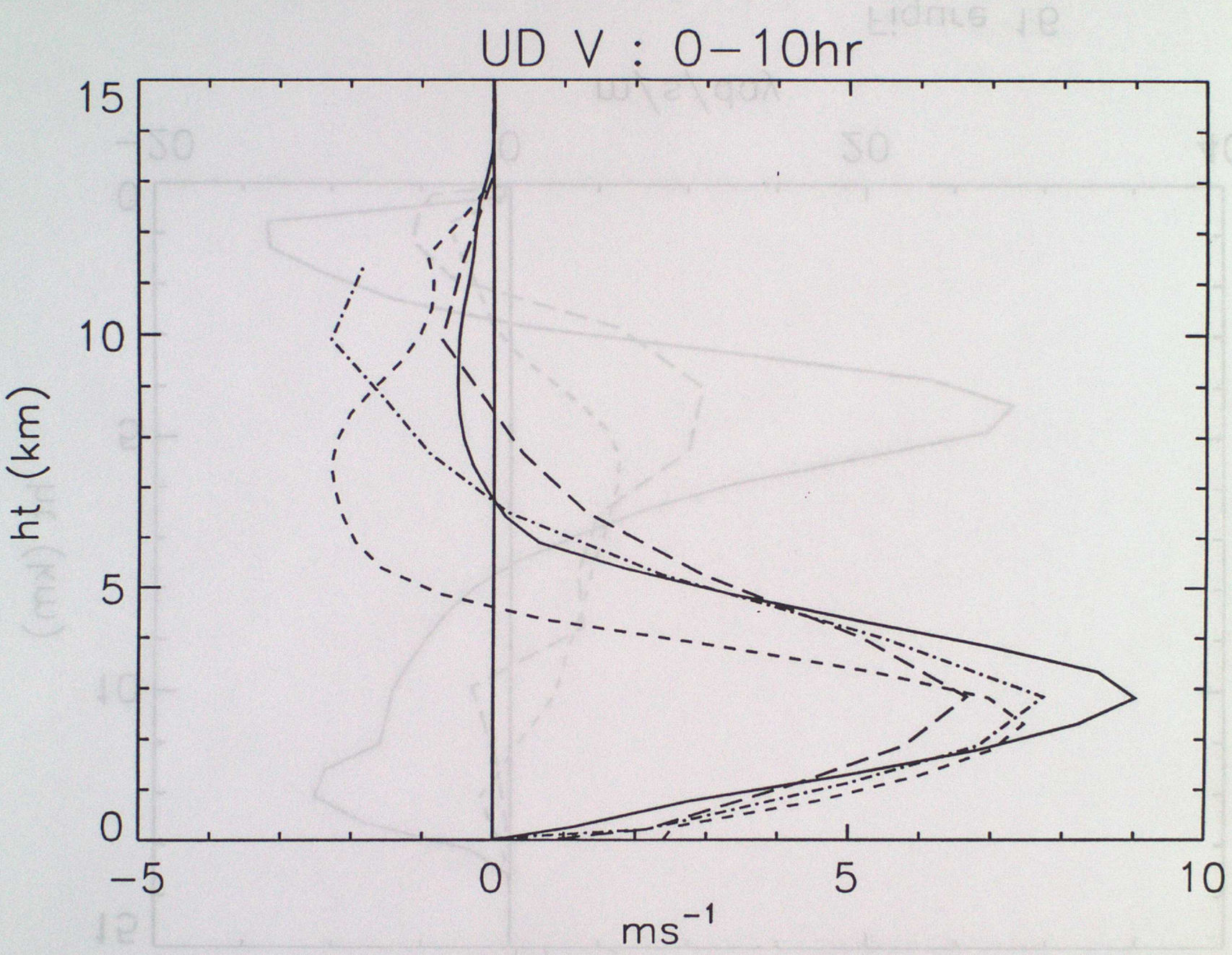

Figure 17

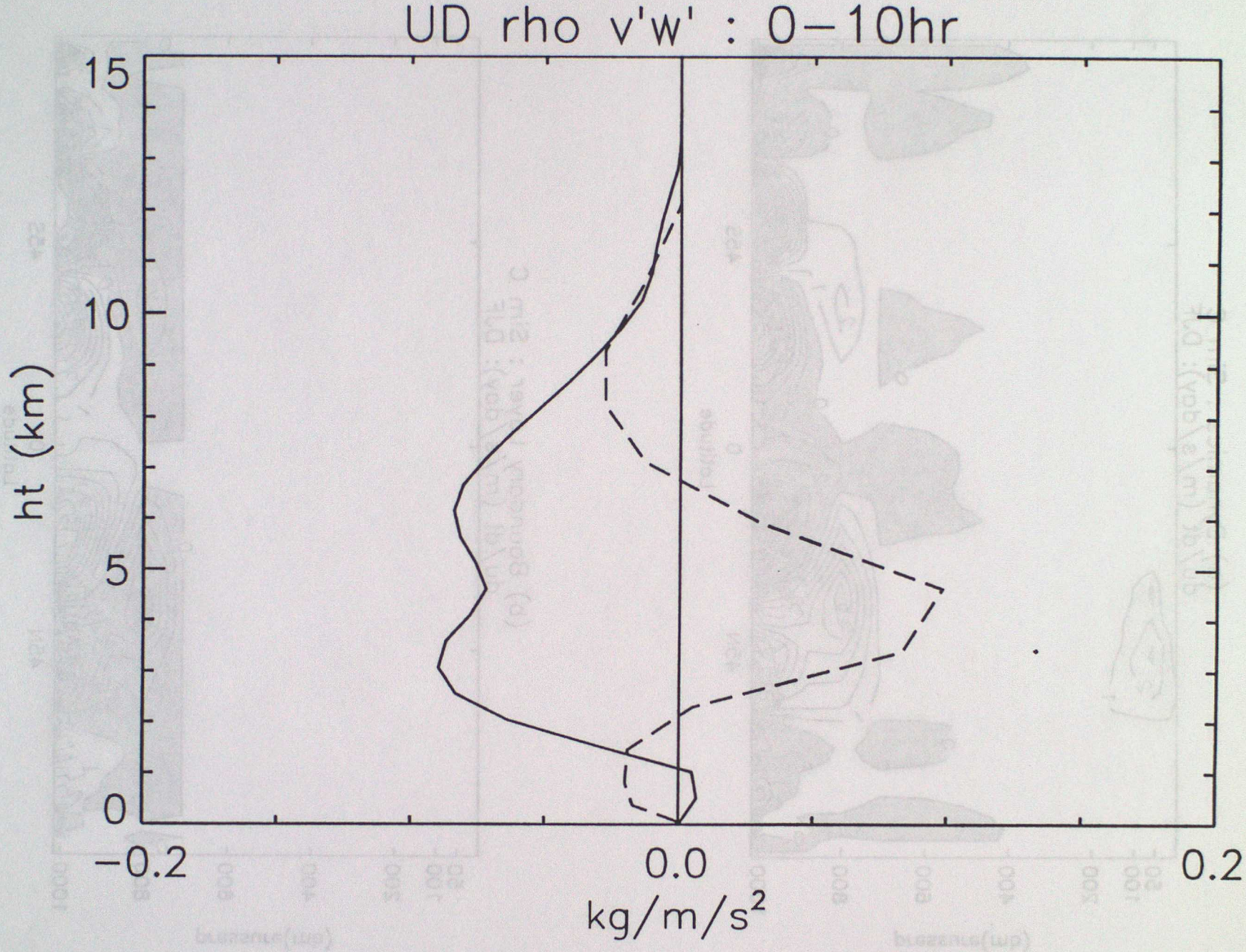

Figure 18

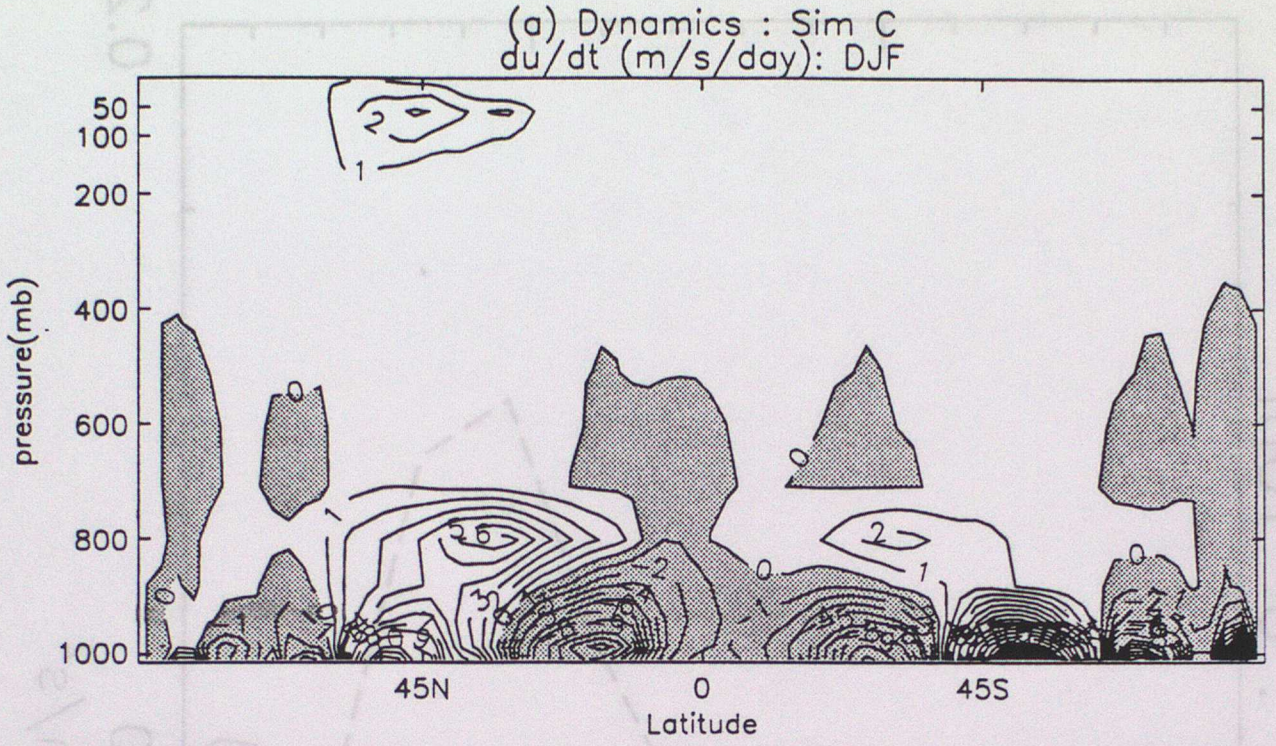
(a) Dynamics : Sim C
du/dt (m/s/day): DJF
pressure(mb)
50
100
200
400
600
800
1000
45N
0
45S
Latitude

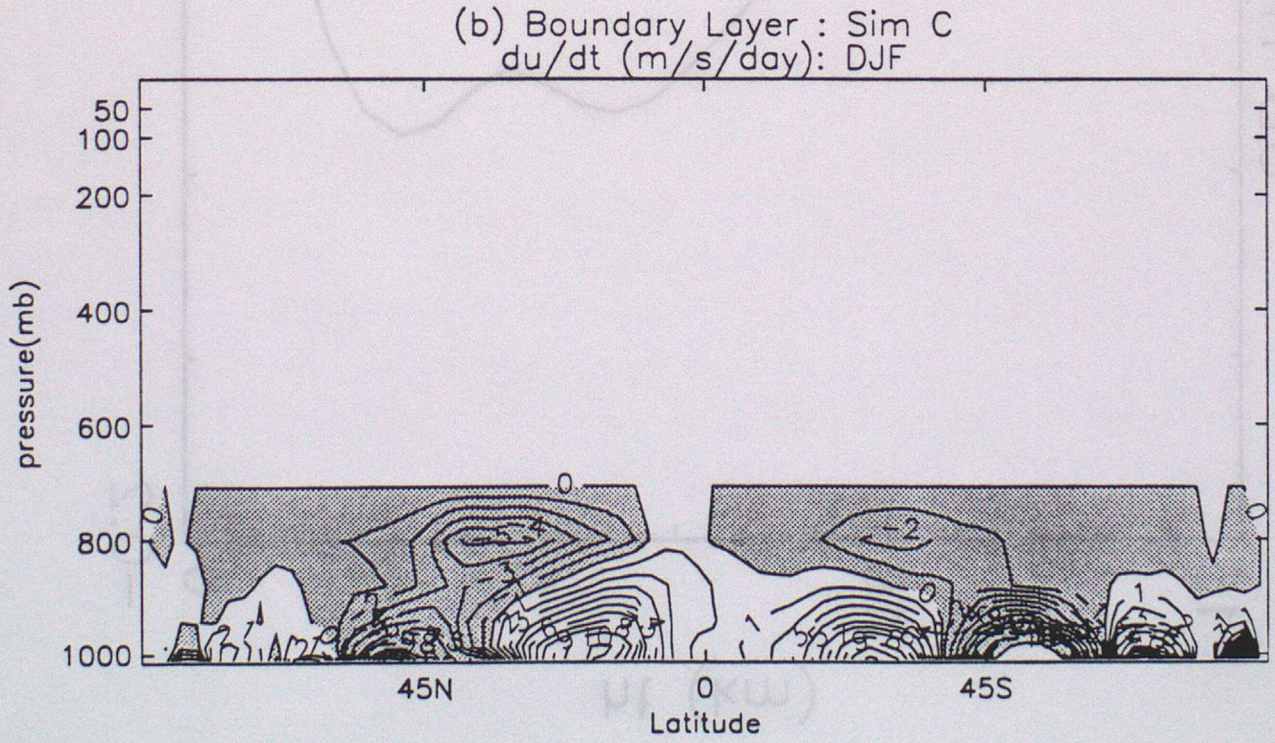
(b) Boundary Layer : Sim C
du/dt (m/s/day): DJF
pressure(mb)
50
100
200
400
600
800
1000
45N
0
45S
Latitude

Figure 19

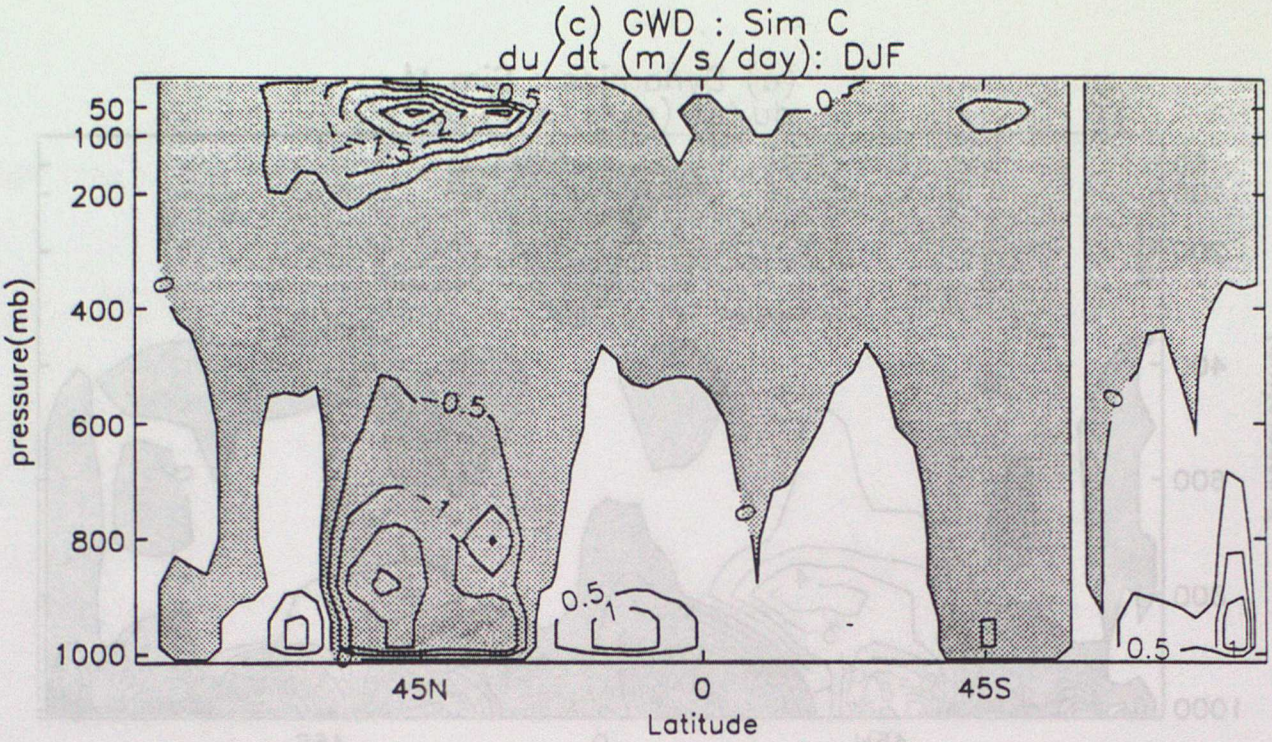

Figure 19 contd

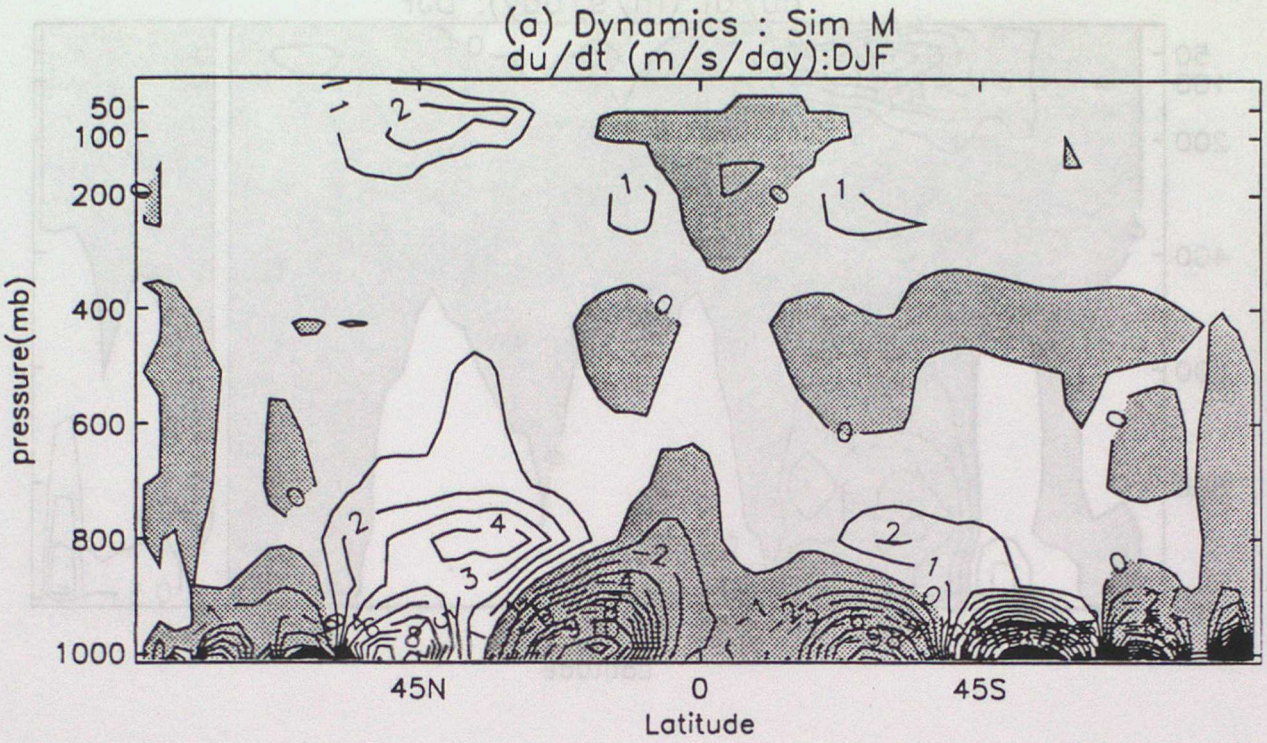
(a) Dynamics : Sim M
du/dt (m/s/day):DJF
pressure(mb)
50
100
200
400
600
800
1000
45N
0
45S
Latitude

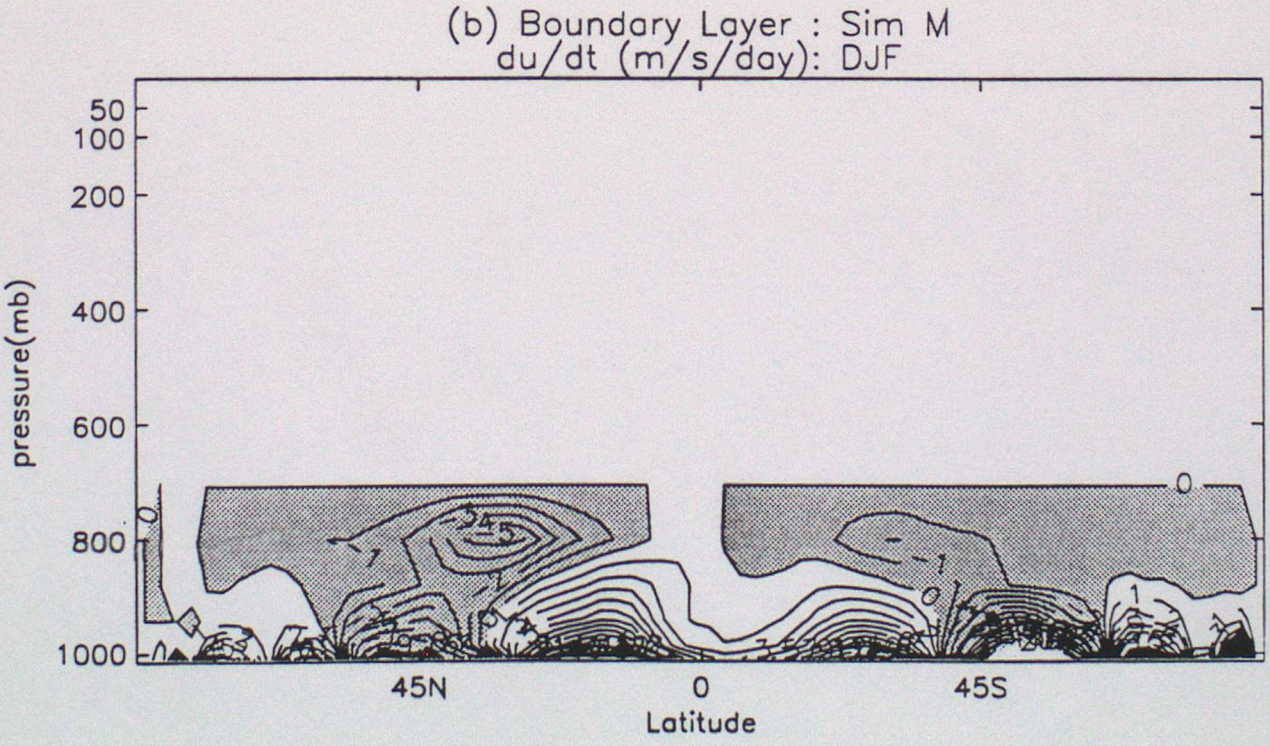
(b) Boundary Layer : Sim M
du/dt (m/s/day): DJF
pressure(mb)
50
100
200
400
600
800
1000
45N
0
45S
Latitude

Figure 20

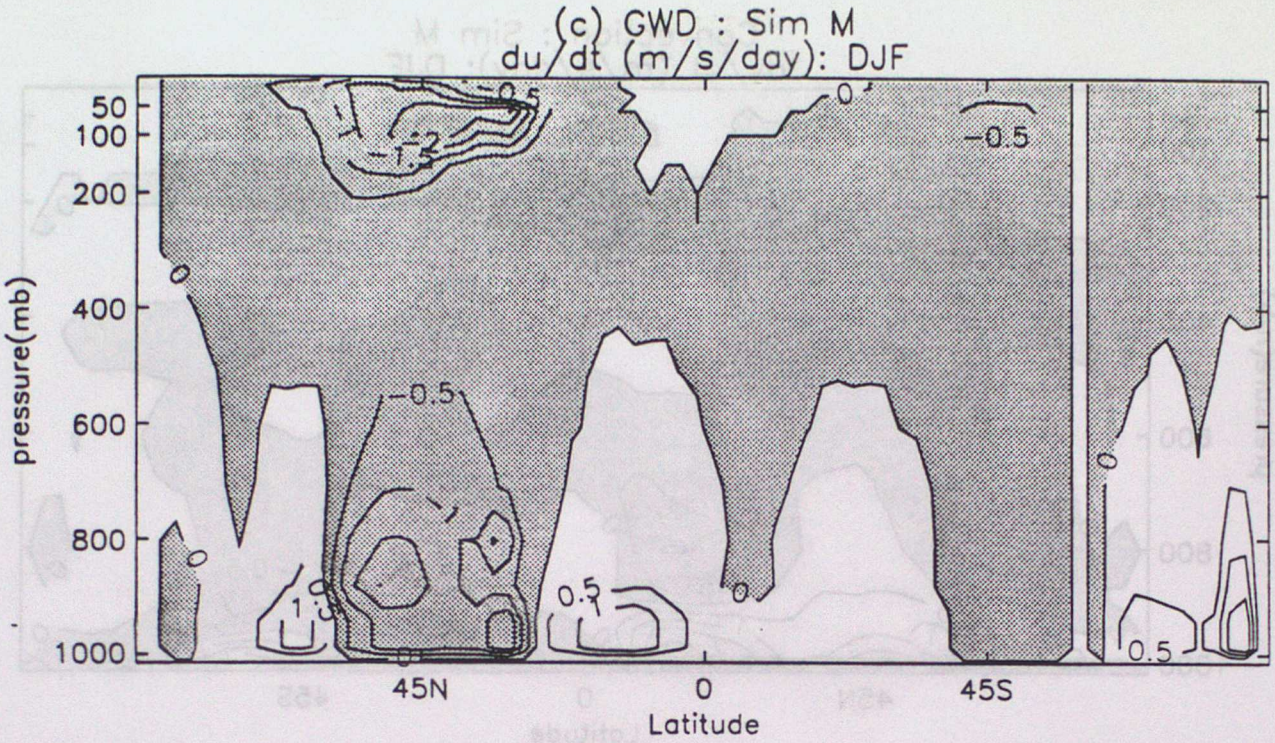

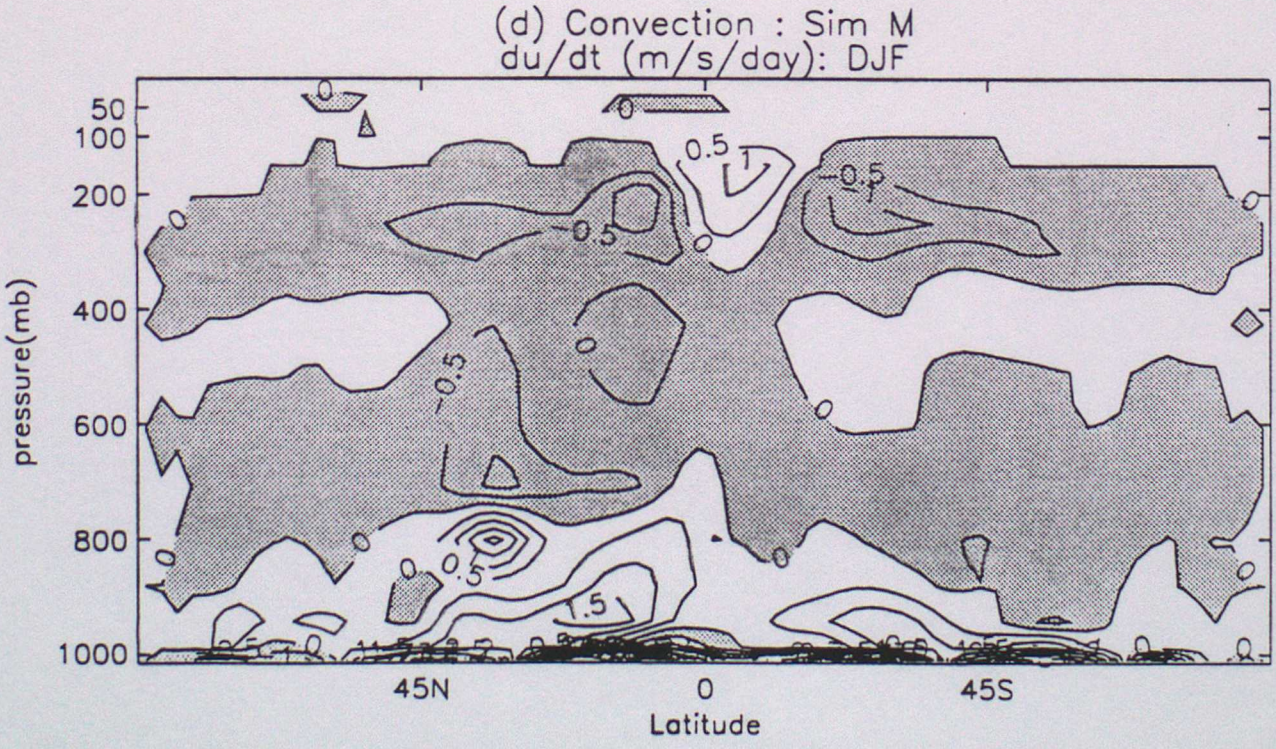

Figure 20 contd

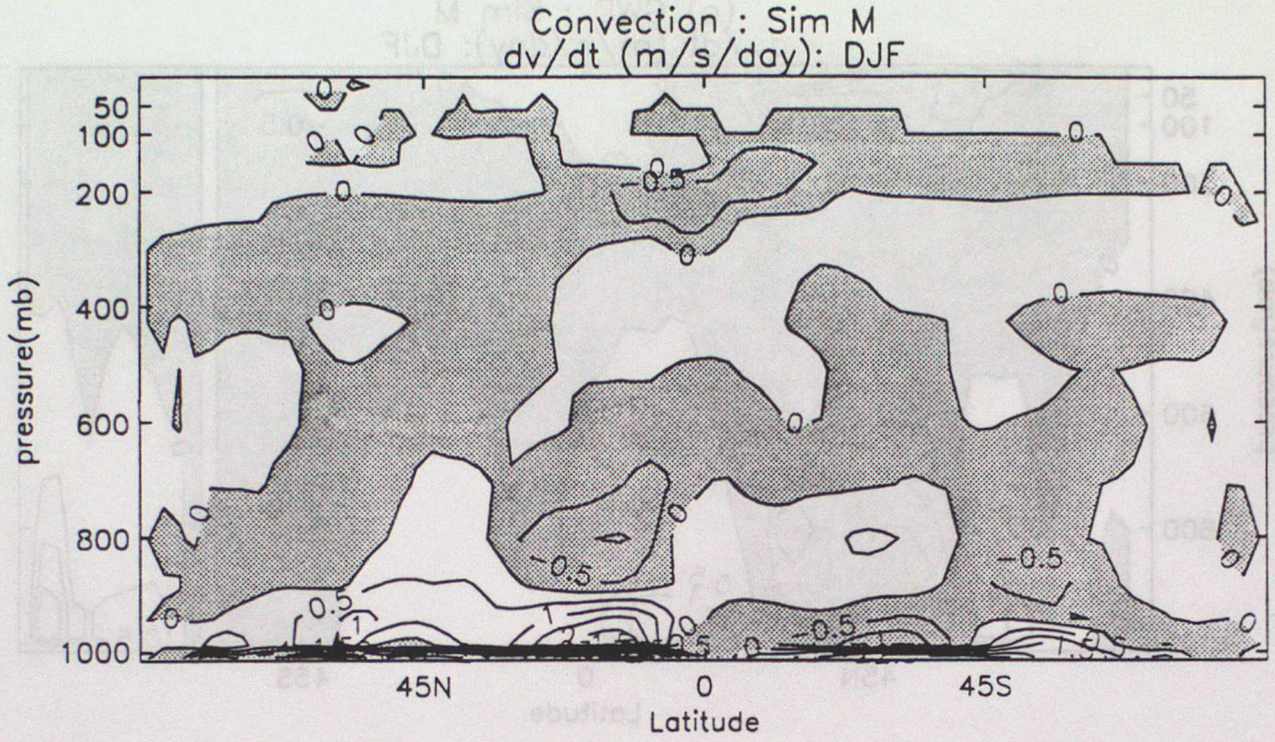
Convection : Sim M
dv/dt (m/s/day): DJF
pressure(mb)
50
100
200
400
600
800
1000
45N
0
45S
Latitude

Figure 21

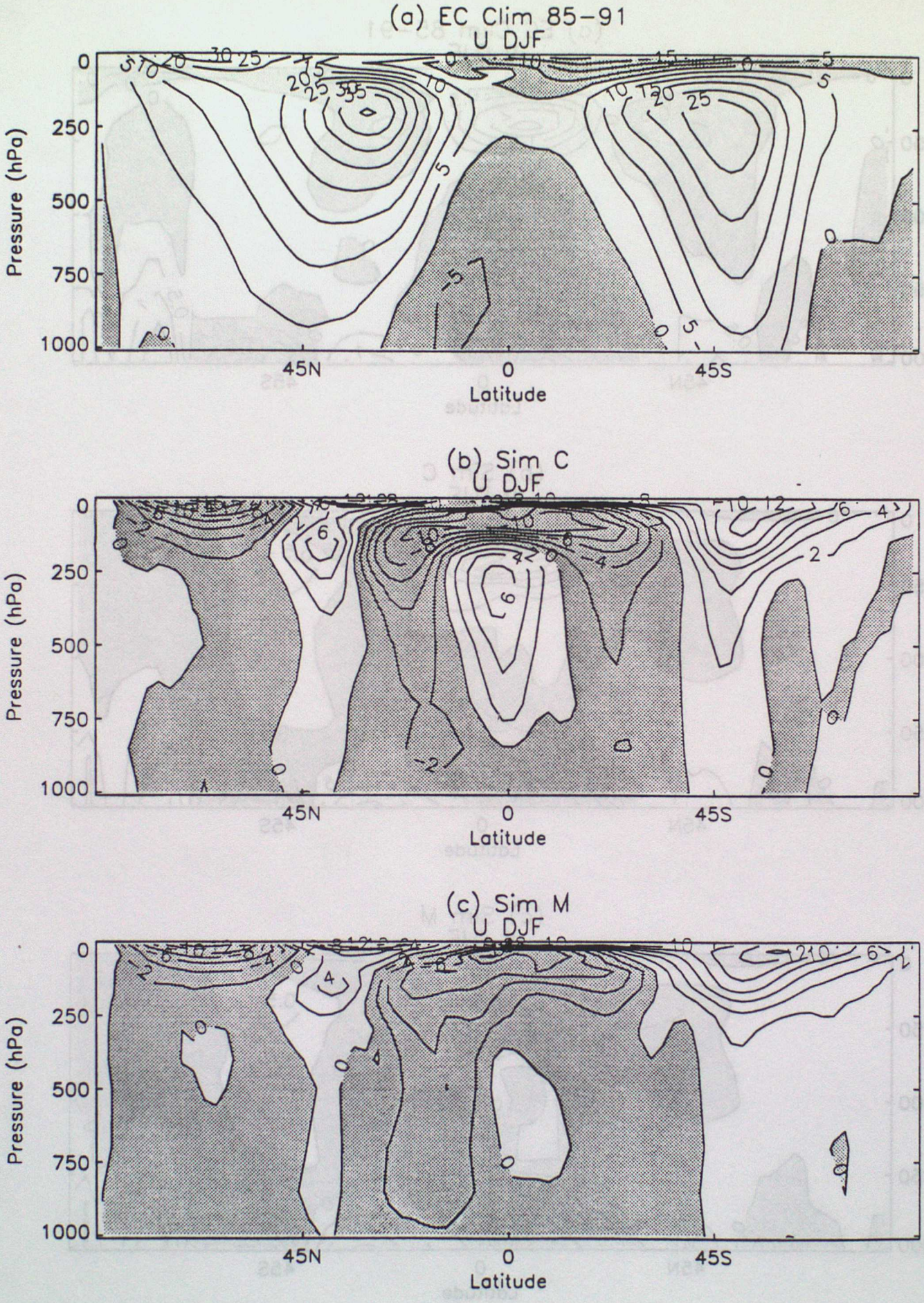
(a) EC Clim 85-91
U DJF
(b) Sim C
U DJF
(c) Sim M
U DJF
Pressure (hPa)
0
250
500
750
1000
45N
0
45S
Latitude

Figure 22

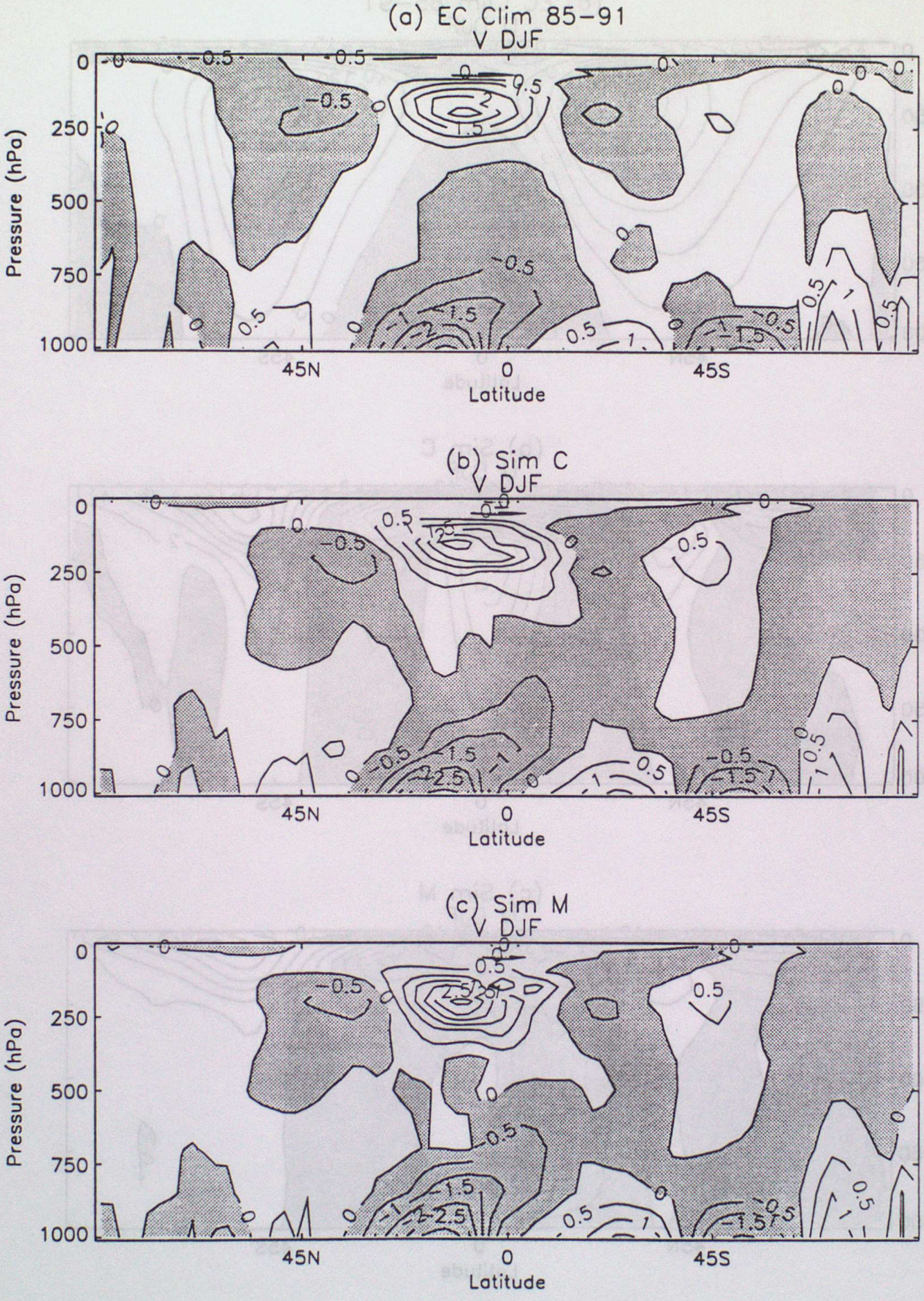
(a) EC Clim 85-91
V DJF
(b) Sim C
V DJF
(c) Sim M
V DJF
Pressure (hPa)
0
250
500
750
1000
45N
0
45S
Latitude

Figure 23

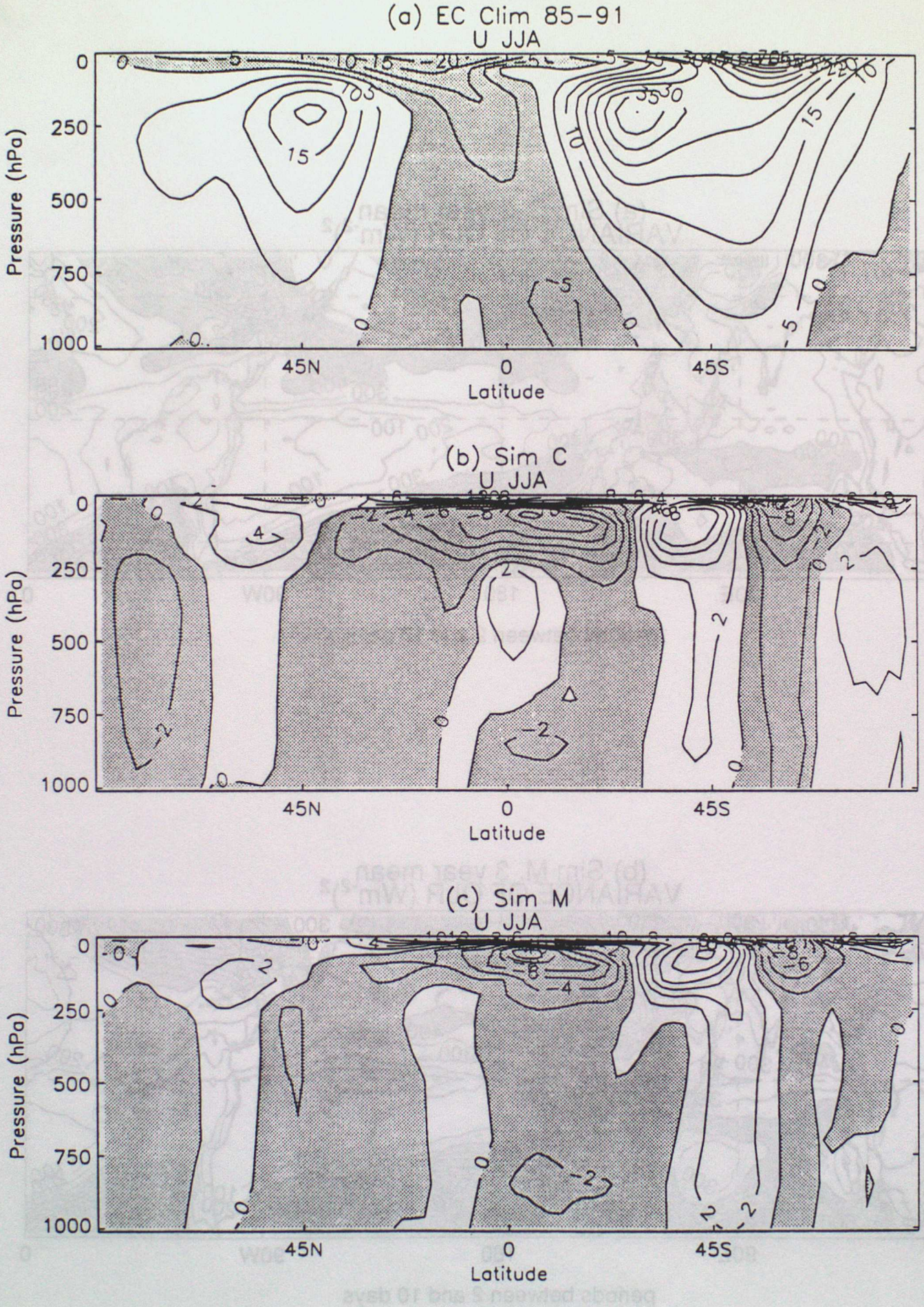
(a) EC Clim 85–91
U JJA
(b) Sim C
U JJA
(c) Sim M
U JJA
Pressure (hPa)
0
250
500
750
1000
45N
0
45S
Latitude

Figure 24

(a) Sim C. 3 year mean
VARIANCE OF OLR $(Wm^{-2})^2$

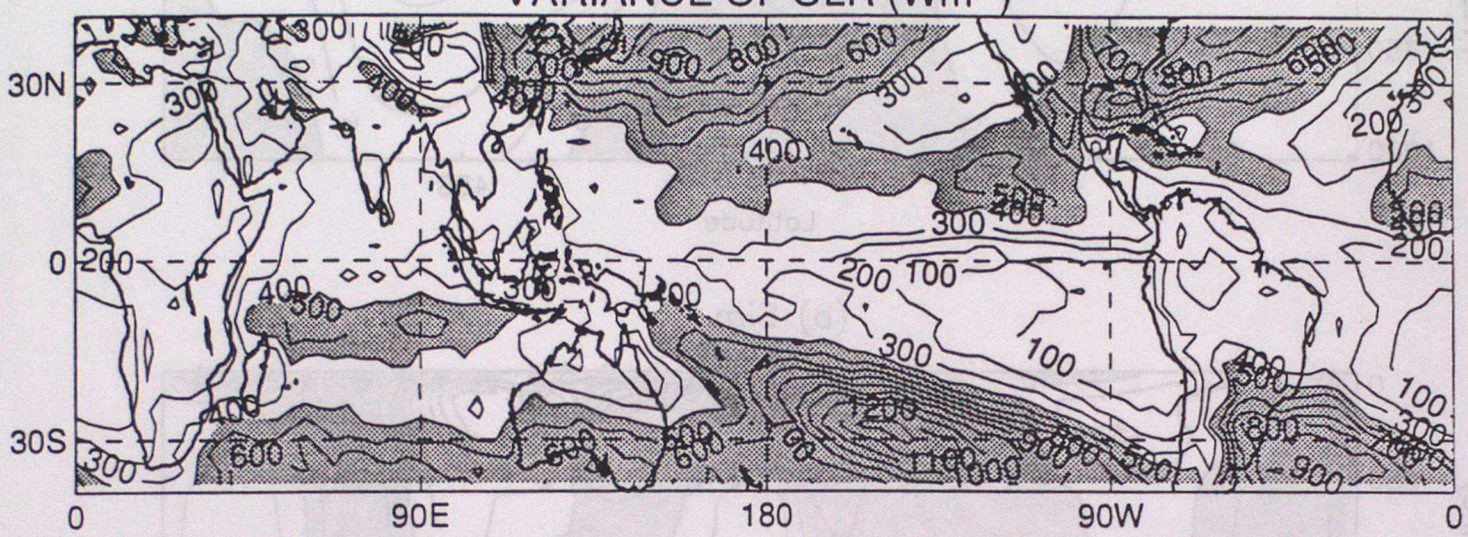

periods between 2 and 10 days

(b) Sim M. 3 year mean
VARIANCE OF OLR $(Wm^{-2})^2$

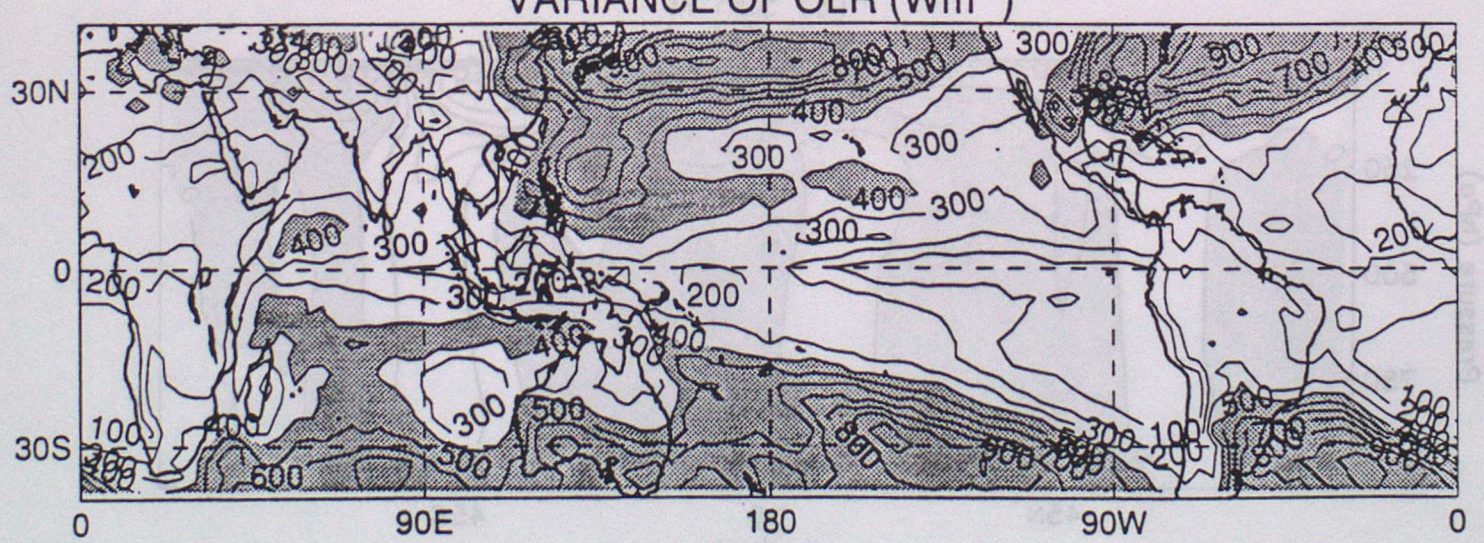

periods between 2 and 10 days

Figure 25

CLIMATE RESEARCH TECHNICAL NOTES

CRTN 1	Oct 1990	Estimates of the sensitivity of climate to vegetation changes using the Penman-Monteith equation. P R Rowntree
CRTN 2	Oct 1990	An ocean general circulation model of the Indian Ocean for hindcasting studies. D J Carrington
CRTN 3	Oct 1990	Simulation of the tropical diurnal cycle in a climate model. D P Rowell
CRTN 4	Oct 1990	Low frequency variability of the oceans. C K Folland, A Colman, D E Parker and A Bevan
CRTN 5	Dec 1990	A comparison of 11-level General Circulation Model Simulations with observations in the East Sahel. K Maskell
CRTN 6	Dec 1990	Climate Change Prediction. J F B Mitchell and Qing-cun Zeng
CRTN 7	Jan 1991	Deforestation of Amazonia - modelling the effects of albedo change. M F Mylne and P R Rowntree
CRTN 8	Jan 1991	The role of observations in climate prediction and research. D J Carson
CRTN 9	Mar 1991	The greenhouse effect and its likely consequences for climate change. D J Carson
CRTN 10	Apr 1991	Use of wind stresses from operational N.W.P. models to force an O.G.C.M. of the Indian Ocean. D J Carrington
CRTN 11	Jun 1991	A new daily Central England Temperature series, 1772-1991. D E Parker, T P Legg and C K Folland
CRTN 12	Jul 1991	Causes and predictability of Sahel rainfall variability. D P Rowell, C K Folland, K Maskell, J A Owen, M N Ward

CLIMATE RESEARCH TECHNICAL NOTES

CRTN 13	Jul 1991	Modelling changes in climate due to enhanced CO2, the role of atmospheric dynamics, cloud and moisture. C A Senior, J F B Mitchell, H Le Treut and Z-X Li
CRTN 14	Sep 1991	Sea temperature bucket models used to correct historical SST data in the Meteorological Office. C K Folland
CRTN 15	Aug 1991	Modelling climate change, and some potential effects on agriculture in the U.K. P R Rowntree, B A Callander and J Cochrane
CRTN 16	Aug 1991	The Boreal Forests and Climate G Thomas and P R Rowntree
CRTN 17	Aug 1991	Development of a Stratosphere-Troposphere Data Assimilation System. R Swinbank.
CRTN 18	Sep 1991	A study of asynchronous coupling using a simple climate model. M K Davey.
CRTN 19	Sep 1991	The Oceanic Carbon Cycle. N K Taylor
CRTN 20	Nov 1991	Worldwide ocean-atmosphere surface fields in Sahel wet and dry years using provisionally corrected surface wind data. M N Ward
CRTN 21	Dec 1991	Coupled tropical ocean global atmosphere models at the UKMO. M K Davey, C Gordon, S Ineson and S Lawrence
CRTN 22	Dec 1991	Empirical parameterisation of tropical ocean-atmosphere coupling. M Allen, M K Davey, D L T Anderson and P D Killworth
CRTN 23	Feb 1992	The temporal evolution of Equatorial Currents in the Indian Ocean D L T Anderson, D J Carrington, R A Corry and C Gordon
CRTN 24	Feb 1992	Stratospheric analyses provided by the U.K. Meteorological Office M J Bailey, A O'Neill and V D Pope

CLIMATE RESEARCH TECHNICAL NOTES

CRTN 25	Feb 1992	Modelling interannual variability in the Indian Ocean using momentum fluxes from the UKMO and ECMWF operational weather analyses. D L T Anderson and D J Carrington
CRTN 26	Mar 1992	A GCM simulation of the impact of Amazonian deforestation on climate using an improved canopy representation J Lean and P R Rowntree
CRTN 27	Mar 1992	The parameterization of rainfall interception in GCMs A J Dolman and D Gregory
CRTN 28	Jun 1992	Development of worldwide marine data eigenvectors since 1985 A W Colman
CRTN 29	Jun 1992	A tropical ocean model with reduced physics M K Davey
CRTN 30	Jun 1992	International Temperature Workshop, Boulder, Colorado, USA, 16 January 1992 Edited by D E Parker
CRTN 31	Jul 1992	Simulation of clear-sky outgoing longwave radiation over the oceans using operational analyses A Slingo and M J Webb
CRTN 32	Sep 1992	A prediction of the transient response of climate J M Murphy
CRTN 33	Nov 1992	LEPS scores for assessing climate model simulations and long-range forecasts. C K Folland
CRTN 34	Jan 1993	Stratospheric Data Assimilation System Guide Editer: R Swinbank
CRTN 35	Mar 1993	A Stratosphere-Troposphere Data Assimilation System R Swinbank and A O'Neill
CRTN 36	Mar 1993	Validation of hydrological schemes for climate models against catchment data. P R Rowntree and J Lean

CLIMATE RESEARCH TECHNICAL NOTES

CRTN 37	Apr 1993	Modelling of palaeoclimates: Examples from the recent past J F B Mitchell
CRTN 38	May 1993	A simulation of seasonality in ENSO forecast skill M K Davey, D L T Anderson and S Lawrence
CRTN 39	Jul 1993	ENSO Prediction experiments using a simple ocean-atmosphere model D-H Wu, D L T Anderson and M K Davey
CRTN 40	Sep 1993	Diagnosis of dynamic sea-surface and sea-level changes from the Cox ocean model J M Gregory
CRTN 41	Sep 1993	Seasonal variations of the clear-sky greenhouse effect: the role of changes in atmospheric temperatures and humidities M J Webb, A Slingo and G L Stephens
CRTN 42	Nov 1993	Sea-level changes under increasing atmospheric CO_2 in a transient coupled ocean-atmosphere GCM experiment. J M Gregory
CRTN 43	Dec 1993	Global and regional patterns of climate change: recent predictions for the Arctic P R Rowntree
CRTN 44	Feb 1994	The effect of changing horizontal diffusion in the atmospheric version of the unified climate model C D Hall and R A Stratton
CRTN 45	Mar 1994	Simulation of El-Niño/Southern Oscillation like variability in a global AOGCM and its response to CO_2 increase. S F B Tett
CRTN 46	Apr 1994	Global data required for monitoring climate change. D E Parker and C K Folland
CRTN 47	May 1994	Seasonal uptake of anthropogenic CO_2 in an ocean general circulation model. N K Taylor

CLIMATE RESEARCH TECHNICAL NOTES

CRTN 48	Jun 1994	A tropic-wide oscillation of boreal summer rainfall and patterns of sea-surface temperature. M N Ward, K Maskell, C K Folland, D P Rowell and R Washington
CRTN 49	Jun 1994	Simulation of the tropical Pacific using a simplified ocean model M A Balmaseda, D L T Anderson and M K Davey
CRTN 50	Sep 1994	Simulation of global mean temperature using a box-diffusion climate model P R Rowntree
CRTN 51	Sep 1994	Seasonal dependence of ENSO prediction skill M A Balmaseda, M K Davey and D L T Anderson
CRTN 52	Nov 1994	Simulation of the Indian Monsoon and Tropical Intraseasonal Variability by a General Circulation Model P M Inness and D Gregory
CRTN 53	Mar 1995	A comparison of modelled surface fluxes with climatological estimates. C Gordon and D K Wright
CRTN 54	Mar 1995	The representation of moist convection in atmospheric models. D Gregory
CRTN 55	Mar 1995	A consistent treatment of the evaporation of rain and snow for use in large-scale models D Gregory
CRTN 56	Apr 1995	Workshop on simulations of the Climate of the Twentieth Century using GISST, 28-30 November 1994, Hadley Centre, Bracknell, UK Edited by C K Folland and D P Rowell
CRTN 57	May 1995	Enhanced shortwave cloud radiative forcing due to anthropogenic aerosols. S E Swartz and A Slingo
CRTN 58	May 1995	The simulation of the tropical oceans in models of different horizontal resolution. C Gordon, D K Wright and C M Roberts
CRTN 59	Sep 1995	The water budget of middle latitude continental regions - a modelling and observational study P R Rowntree
CRTN 60	Sep 1995	Intraseasonal variability of the Indian summer monsoon simulated by the Hadley Centre climate model K Ashok, D Gregory and P M Inness

CLIMATE RESEARCH TECHNICAL NOTES

CRTN 61	Sep 1995	Climate simulations with the Unified Model: AMIP runs C D Hall, R A Stratton and M L Gallani
CRTN 62	Nov 1995	Validation of surface parameters over the oceans in climate simulations with the unified model. C D Hall
CRTN 63	Dec 1995	The GISST2.2 sea surface temperature and sea-ice climatology D E Parker, M Jackson and E B Horton
CRTN 64	Dec 1995	Parametrization of momentum transport by convection. II: Tests in single column and general circulation models. D Gregory, R Kershaw and P M Inness